

Review

A comprehensive review on the state-of-the-art of piezoelectric energy harvesting

Nurettin Sezer^{*}, Muammer Koç*Division of Sustainable Development, College of Science and Engineering, Hamad Bin Khalifa University, Qatar Foundation, Education City, Doha, Qatar*

ARTICLE INFO

Keywords:
 Piezoelectric effect
 Ceramic
 Polymer
 Composite
 Piezoelectric coefficient
 Piezoelectric applications

ABSTRACT

The global energy crisis and environmental pollutions caused mainly by the increased consumption of non-renewable energy sources prompted researchers to explore alternative energy technologies that can harvest energies available in the ambient environment. Mechanical energy is the most ubiquitous ambient energy that can be captured and converted into useful electric power. Piezoelectric transduction is the prominent mechanical energy harvesting mechanism owing to its high electromechanical coupling factor and piezoelectric coefficient compared to electrostatic, electromagnetic, and triboelectric transductions. Thus, piezoelectric energy harvesting has received the utmost interest by the scientific community. Advancements of micro and nanoscale materials and manufacturing processes have enabled the fabrication of piezoelectric generators with favorable features such as enhanced electromechanical coupling factor, piezoelectric coefficient, flexibility, stretch-ability, and integrate-ability for diverse applications. Besides that, miniature devices with lesser power demand are realized in the market with technological developments in the electronics industry. Thus, it is anticipated that in near future, many electronics will be powered by piezoelectric generators. This paper presents a comprehensive review on the state-of-the-art of piezoelectric energy harvesting. The piezoelectric energy conversion principles are delineated, and the working mechanisms and operational modes of piezoelectric generators are elucidated. Recent researches on the developments of inorganic, organic, composite, and bio-inspired natural piezoelectric materials are reviewed. The applications of piezoelectric energy harvesting at nano, micro, and mesoscale in diverse fields including transportation, structures, aerial applications, in water applications, smart systems, microfluidics, biomedical, wearable and implantable electronics, and tissue regeneration are reviewed. The advancements, limitations, and potential improvements of the materials and applications of the piezoelectric energy harvesting technology are discussed. Briefly, this review presents the broad spectrum of piezoelectric materials for clean power supply to wireless electronics in diverse fields.

1. Introduction

Today, miniaturization, multifunctionality, portability, flexibility, high computational capability, and low power communication have become the general trend in the development of electronic devices [1–4]. Harvesting the energies available in the ambient environment such as mechanical vibrations, heat, fluid flows, electromagnetic radiation in the form of light and radio waves (RF), and in vivo energies can supply clean power to operate various electronic devices such as wireless sensor networks, mobile electronics, wearable and implantable biomedical devices. These devices have been conventionally powered by electrochemical batteries. However, the life of batteries is limited and oftentimes shorter than the life of electronic devices. Hence, it brings the extra cost of recharging or replacement. In the case of biomedical

devices, additional surgeries are performed for replacing the batteries, which brings about an increased risk of infection and morbidity to the patients, as well as an increased economic burden on healthcare institutions. Another drawback of batteries is that they are bulky and usually dominate the weight and size of electronics, which hinders the miniaturization of the devices. Considering all these drawbacks, significant research and developmental efforts have been devoted to the advancement of energy harvesting technologies as a self-power source of a broad range of wireless electronic devices.

Harvesting parasitic energy available in the ambient environment surrounding the electronic device would be a better alternative to the implementation of the conventional batteries as a power source [5,6]. Energies generated by industrial machinery, vehicles during transportation, structures, natural sources, human activities, and movement

* Corresponding author.

of body organs can be captured and converted into useful electric power without affecting the original source. Further, such energy harvesting would allow operation in harsh environments that would not be possible with conventional batteries e.g. temperature above 60 °C. Various energy harvesting strategies have been proposed using electromagnetic, electrostatic, piezoelectric, triboelectric, thermoelectric, and pyroelectric transduction mechanisms at meso, micro, and nanoscale [7]. Among them, piezoelectric harvesters employ active materials to convert mechanical strains into electric power, whereas electrostatic, triboelectric, and electromagnetic harvesters generate electric power through varying capacitance, frictional contact and electrostatic induction, and magnetic induction, respectively. Heat is another valuable source for ambient energy harvesting. Thermoelectric and pyroelectric energy harvesters generate electric power on the basis of the available temperature gradient and thermal fluctuations, respectively.

Among all the ambient energy sources, mechanical energy is the most ubiquitous energy that can be captured and converted into useful electric power [5,8–11]. Piezoelectric energy harvesting is a very convenient mechanism for capturing ambient mechanical energy and converting it into electric power since the piezoelectric effect is solely based on the intrinsic polarization of the material and it does not require a separate voltage source, magnetic field, or contact with another material as in the case of electrostatic, electromagnetic, and triboelectric energy harvesting, respectively [12,13]. Piezoelectric generators are durable, reliable, more sensitive to minute strains, and exhibit ~3–5-fold higher density power output and higher voltage output compared to the other energy harvesting methods [14–19]. Moreover, piezoelectric generators can be manufactured in small dimensions and compact structures, and easily integrated into microelectromechanical systems. Further, they are not affected by environmental factors such as humidity [1,8,20,21]. Thus, piezoelectric transduction is the most promising ambient energy harvesting technology that has found applications in many diverse fields including structures, transportation, wireless electronics, microelectromechanical systems, Internet of Things (IoT), wearable and implantable biomedical devices, and so on [22].

A number of piezoelectric materials such as single crystals, ceramics, polymers, composites, and bio-inspired materials have been prepared in the form of the nanostructure, thin-film, and layer stacks for building piezoelectric generators to be deployed in a number of fields. The prominent field of application of piezoelectric generators is the wireless sensor networks. The continuous increase in the number of sensor nodes deployed in diverse fields and the significant reduction of node size and power requirement made it convenient to harvest ambient energy for sustainable power supply to the sensor nodes. Transportation, avionics, defense, infrastructure, environmental monitoring, networking, electronics, healthcare, and many other industries are the potential field of application of piezoelectric energy harvesters. For instance, the pressure of a tire can be monitored by wireless communication of sensors powered by piezoelectric energy harvesters. Snyder [23,24] patented the use of piezoelectric generators embedded in the car wheels to power tire pressure sensors. The generator was powered by the vibration of the wheel during driving, and abnormal tire pressure was reported to the driver through a low-power radio link. Another example of the energy harvesting in transportation is the prediction of the failure of rail wheel bearings by the wireless communication of piezoelectric sensors that convert the vibration of rolling stock into electrical power [25].

Piezoelectric generators can make use of the in vivo energies, too such as the beat of a heart, lung motion, muscle stretching, and blood flow for powering biomedical devices such as a cardiac pacemaker, deep brain stimulator, hearing aids, or sensors for diagnosing heart rate, blood pressure, respiration, and so on for a number of diseases related to the heart, brain, and other important organs [26–28].

Aside from in vivo energies, the biomechanical energy generating from the physical activities such as footfalls, hand swings, and finger tapping, etc. can be used by deploying piezoelectric energy harvesters on footwears, knees, elbows, wrists, and fingers to power a number of

electronic devices such as LED lights, wristwatches, mobile phones, and implantable biomedical devices [29]. Besides, the biomechanical energy of wild animals or livestock on a farm can power electronic devices for monitoring their health status. The ambient mechanical energy is also utilized to self-power sensor nodes for environmental monitoring such as humidity and dust through the piezoelectric effect [30,31].

The recent research and developmental efforts on piezoelectric materials and manufacturing methods at micro and nanoscale have enabled widening the application fields of piezoelectric technology. Newly developed piezoelectric materials such as ceramics, polymers, composites, and bio-inspired natural materials in the form of different nanostructures and thin films with satisfactory physical properties such as high piezoelectric coefficient, flexibility, stretchability, and durability favored their use in emerging fields including wireless sensor networks, IoT, wearable electronics, and implantable biomedical devices. Thus, piezoelectric energy harvesting has received a growing interest worldwide. The number of documents within this context has tremendously raised from 1 to 1172 by the time between 2000 and 2019 (Fig. 1). In the meantime, excellent review papers have been published based on various aspects of piezoelectric energy harvesting such as materials [32–34], device architectures [35], circuit designs [36], energy sources [37–39], applications [35,40], and performance optimization [41]. Despite the availability of literature reviews that specifically focus on some of the abovementioned aspects of piezoelectric energy harvesting, none of the recent reviews compiles the broad spectrum of materials and applications in one literature. The present paper is a comprehensive review on the state-of-the-art of piezoelectric energy harvesting. It is specifically aimed to compile, discuss, and summarize the recent literature on materials and applications of piezoelectric energy harvesting. Firstly, concise background information on electromechanical energy harvesting, piezoelectric transduction mechanism, energy harvesting device structures, and operation modes is provided in the following sections. Next, a detailed review of a range of piezoelectric materials including ceramics, polymers, composites, and bio-inspired natural materials is presented. Finally, the applications of piezoelectric generators in diverse fields such as transportation, structures, aerial applications, in water applications, smart systems, microfluidics, biomedical, wearable and implantable electronics, and neuronal and bone tissue regeneration are reviewed. Briefly, this paper is an up-to-date review of piezoelectric energy harvesting with an emphasis on the broad spectrum of materials and applications.

2. Electromechanical energy harvesting

Mechanical energy is the most ubiquitous and versatile energy available in the ambient environment. Motion, flow, and the vibration of a source can be captured and converted into electrical power through mechanical-to-electrical transduction [42].

Inertial energy harvesting is the widely implemented method in electromechanical energy harvesting, which relies on the resistance of a mass to acceleration. In the literature, vibration energy harvesting is extensively studied by incorporating a basic configuration of spring-mass-damping system, which represents the inertial energy harvesters [4]. The system consists of a seismic mass, "m" and a spring with a stiffness "k". When the generator moves with a displacement "y(t)", a vibration is set up in the mass-spring system. The mass moves out of phase with the frame that produces a relative movement between the mass and frame; "z(t)" (Fig. 2). The resultant sinusoidal displacement is converted into electrical energy via piezoelectric transduction. Each inertial system has a certain resonant frequency that is designed to match the frequency of the vibration source. The amplitude of the vibration in the mass-spring system is significantly larger than the amplitude of the frame. Energy losses within the system comprising parasitic losses, " b_p ", and electrical power extracted by the transduction mechanism, " b_e " are represented by the damping coefficient, "b". These components are associated with the excitation of the inertial frame by

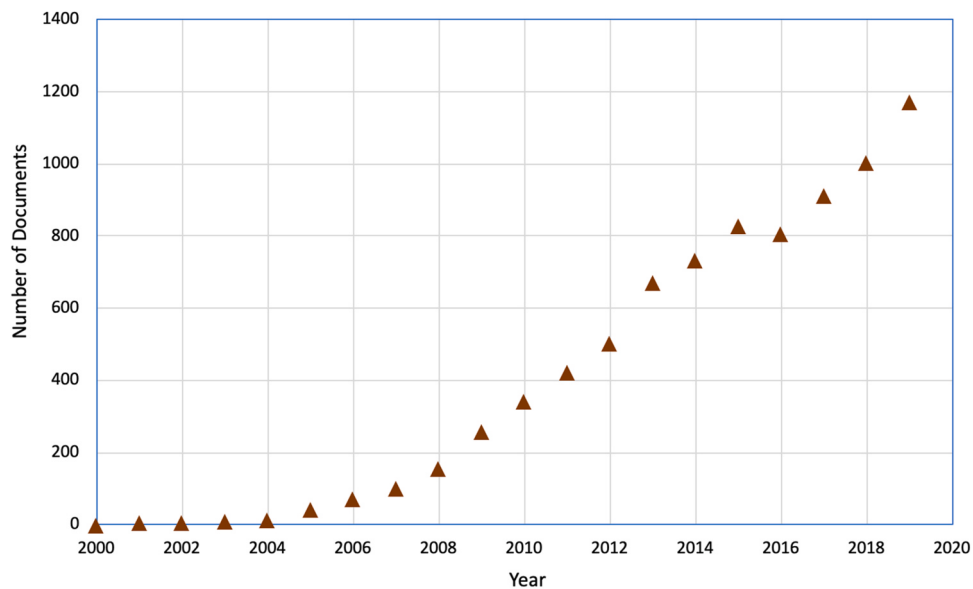


Fig. 1. Number of documents on “piezoelectric energy harvesting” by year (all data from Scopus).

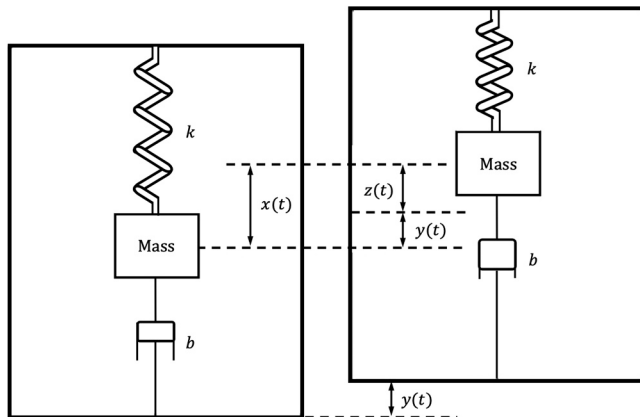


Fig. 2. Spring-mass system for mechanical energy harvesting [43].

sinusoidal vibration of the form $y(t) = Y\sin(\omega t)$ where “Y” is amplitude and “ ω ” is the angular frequency of vibration. The piezoelectric transduction mechanism generates electricity by exploiting the mechanical strain. Active piezoelectric materials are employed to convert deformation into electrical power.

3. Piezoelectric transduction mechanism

The piezoelectric effect was first discovered by Pierre and Jacques Curie brothers in 1880. It is described as the asymmetric shift of charges or ions of piezoelectric materials when exposed to mechanical strain. Certain crystalline materials such as quartz, barium titanate, topaz, Rochelle salt (sodium potassium tartrate tetrahydrate $[(\text{NaK}_2\text{C}_4\text{H}_4\text{O}_6 \cdot 4\text{H}_2\text{O})]$), tourmaline, as well as natural organic materials such as cane sugar exhibit piezoelectricity that generate electricity under the effect of applied pressure. As such, a direct piezoelectric effect is achieved. The converse piezoelectric effect is attained if the electric potential is applied to the same materials to undergo mechanical deformation as illustrated in Fig. 3. Both effects are useful in diverse applications; specifically, the direct effect is used as a sensor and energy

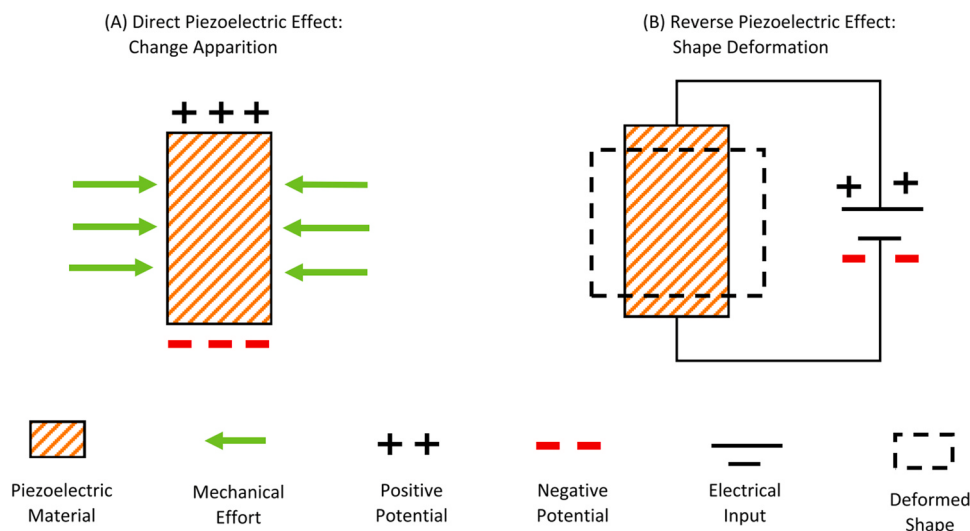


Fig. 3. Electromechanical conversion of piezoelectric phenomena [22].

transducer while the converse effect is used as an actuator [18,44]. The constitutive equations of direct and converse piezoelectric effect are as follows [45].

$$D = dT + \epsilon E \quad (\text{Direct effect}) \quad (1)$$

$$X = sT + dE \quad (\text{Converse effect}) \quad (2)$$

where D is electrical displacement, d piezoelectric coefficient, T stress, ϵ permittivity of the material, E electric field, X strain, and s mechanical compliance.

4. Energy harvesting device structures

The cantilever beam with one or two piezoelectric material layers, termed as unimorph or bimorph (Fig. 4a and b), respectively, is the most widely used device structure for piezoelectric energy generators (Fig. 4) since it can produce large mechanical strain during vibration. A seismic mass is usually attached at the tip of the cantilever to adjust the resonant frequency to the available environment frequency, which is usually below 100 Hz. The beam is placed on a vibration source that induces dynamic strain in piezoelectric layers. As such, an alternating voltage is generated through the electrodes covering the piezoelectric material layers [30].

Another piezoelectric device structure is the cymbal structure that was proposed by Newnham et al. [46]. It consists of two metal cymbal-shape endcaps and a piezoelectric disk placed in between them, as shown in Fig. 5. The metal cymbal-shape endcaps enhance the endurance of the piezoelectric disk under high loads. With the presence of a cavity, the metal endcaps serve as a mechanical transformer. Thus, a portion of the incident axial stress is converted into the radial and tangential stresses that amplify the piezoelectric coefficient d_{31} and d_{33} of the generator [47].

Cymbal structure can generate larger power output ($\sim 100 \mu\text{W}$) compared to that of a cantilever structure that enables harvesting of high load mechanical energy. On the contrary, the loss of mechanical input energy and high resonant frequency are the drawbacks of cymbal structure [47].

In addition to the cantilever and cymbal structures, large numbers of thin piezoelectric materials can be arranged together along the direction of the electric field to form a stack structure. This way, the energy output can be effectively improved. Stack structure is a suitable choice for high load applications. However, the complex stacking process in confined

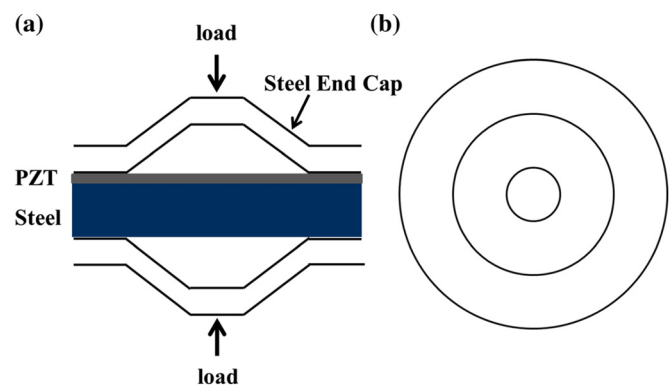


Fig. 5. Schematic illustration of cymbal structure (a) cross-section view and (b) top view [48].

space is the major barrier of stack configuration [47].

5. Operation modes

Piezoelectric materials for energy harvesting usually exhibit a certain polar axis, and the direction of the applied stress relative to the polar axis affects the energy harvesting performance. The polar axis is denoted as "3" direction, and other directions at right angles to the polar axis are denoted as "1" direction. The direction of the applied stress can be either along the polar axis, i.e. 3-direction or at right angles to it i.e. 1-direction, resulting in 33-mode and 31-mode configurations, respectively. These are the two common modes used in piezoelectric energy harvesting as shown in Fig. 6. The applied stress and generated voltage are in the same direction in 33-mode, while in 31-mode, stress is applied in an axial direction, but the voltage is obtained in a perpendicular direction. The open circuit voltage V_{oc} of piezoelectric material is calculated by;

$$V_{oc} = \frac{d_{ij}}{\epsilon_r \epsilon_0} \sigma_{ij} g_e \quad (3)$$

where σ_{ij} is the applied stress, d_{ij} is the piezoelectric coefficient, g_e is the distance between the top and bottom electrodes, ϵ_r is relative dielectric constant, and ϵ_0 is the permittivity. The mode of operation affects the piezoelectric output. The 33-mode yields higher voltage output whereas the 31-mode is superior in high current output [4].

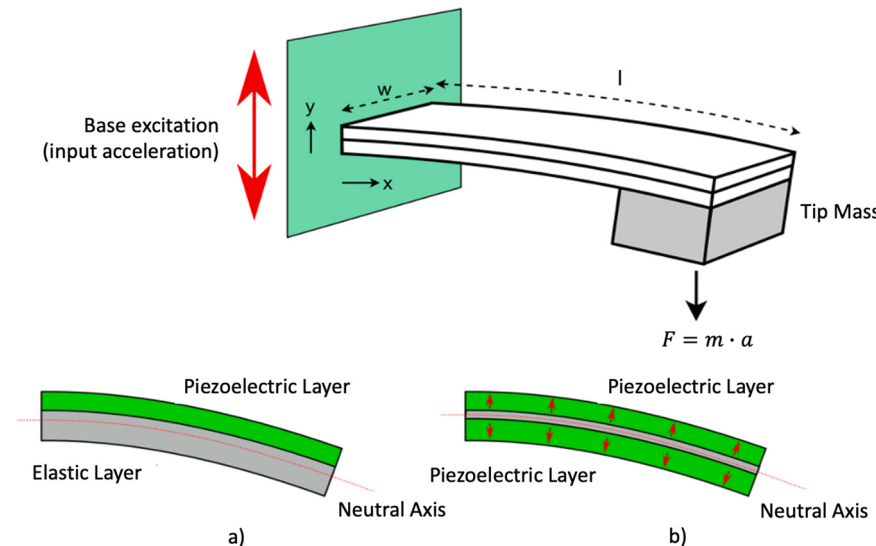


Fig. 4. Cantilever structure of piezoelectric generators with (a) unimorph and (b) bimorph, construction. Reproduced with permission [30] Copyright 2018, John Wiley & Sons, Ltd.

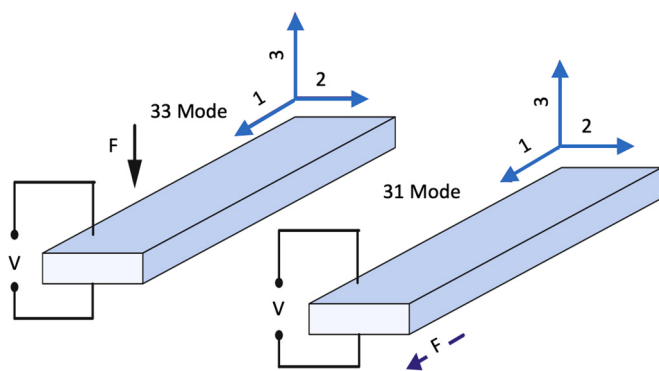


Fig. 6. Operation modes of piezoelectric transducer.

6. Piezoelectric materials

Piezoelectricity is a change in polarization that some materials, such as ferroelectrics, undergo when subjected to mechanical deformation (strain) due to having a crystal structure without a center of symmetry. Piezoelectric materials are active materials that generate electricity in response to minute mechanical strains. The type of material selected for piezoelectric energy harvesting has a major influence on its performance. Therefore, a wide range of materials including inorganic, organic, and composite materials have been investigated for piezoelectric energy harvesting.

Piezoceramics are characterized by their large dielectric and piezoelectric coefficients, and electromechanical coupling factors, as well as high energy conversion rates. However, they are very brittle so they cannot absorb large strains without being damaged. On the contrary, piezopolymers exhibit low electromechanical coupling factor, but they are highly flexible [18]. Piezoelectric composites are another class of materials that combine the benefits of ceramics and polymers required for specific applications.

Piezoelectric materials used in energy harvesting exhibit wurtzite or perovskite crystal structure. Materials with perovskite structure typically exhibit better piezoelectric performance than the wurtzite structure. Nevertheless, an additional process of poling is required to be implemented on materials with the perovskite structure to induce piezoelectric property.

Piezoelectric generators are typically fabricated by sandwiching the prepared piezoelectric materials between elastomeric substrates to induce required flexibility to the generator as well as to protect the piezoelectric layer from environmental factors such as humidity. The top and bottom electrodes are connected to collect the generated electric charge and finally transfer it to the external load.

The important properties of piezoelectric materials for energy harvesting applications include piezoelectric strain constant "d" induced polarization per unit stress applied, voltage constant "g" induced electric field per unit stress applied, electromechanical coupling factor k; square root of the mechanical-electrical energy conversion efficiency, mechanical quality factor "Q" the degree of damping (lower value indicates higher damping), and dielectric constant "ε" the ability of the material to store charge. The values of d, k, and ε for inorganic piezoelectric materials are typically much greater than those of piezoelectric polymers. The g constants of the polymers are higher as they exhibit much lower dielectric constants compared to those of the inorganic materials.

6.1. Inorganic materials

Despite natural materials, such as quartz and berlinitite, exhibit piezoelectricity due to their specific crystalline structure, synthetic materials, such as lead zirconate titanate (PZT) and barium titanate (BT), should be subjected to the poling process to impart piezoelectricity. Perovskite, ilmenite, bismuth-layer, and tungsten bronze

structure ferroelectrics are the most commonly investigated systems that possess the piezoelectric effect. Among these, perovskite is the prominent piezoceramic crystal structure with outstanding performance. Therefore, materials with perovskite structure received the utmost interest from the researchers worldwide. In the perovskite structure, highly symmetrically distributed constitutional atoms allow the deformation of the unit cell easily, which gives rise to various ferroelectrically-active non-cubic phases. The versatility of the perovskite structure is in part based on the many different distortions that the unit cell can undertake.

The first piezoelectric ceramic, BaTiO₃, abbreviated as BT, was discovered in 1947 [49]. It was a revolutionary finding that a polycrystalline material could be rendered permanently piezoelectric after applying an electric field, the so-called poling process. BT was found to have the highest dielectric constant ε_r of 1100 at the time of its development. BT and other later developed class of synthetic ceramic materials were termed as ferroelectrics. The piezoelectric constant (d₃₃) of ferroelectrics was significantly greater than that of natural materials.

Considerable efforts have been devoted to fabricating high-performance BT-based piezoelectric generators. It was found that BT ceramics prepared by using hydrothermal nanoparticles possessed a larger dielectric constant than those fabricated from conventionally synthesized powders [50]. Wada et al. [51] reported that all piezoelectric-related constants of single-crystal BT increased with the decrease of ferroelectric domain size. Takahashi et al. [52] successfully densified hydrothermal nanoparticles by microwave sintering to fabricate high-density and nano-domain BT ceramics that had a dielectric constant of 4200, piezoelectric constant d₃₃ = 350 pC/N, and electromechanical coupling factor k_p = 36%. Besides, Polotai et al. [53] and Wang et al. [54] reported a novel approach to sintering nanocrystalline BT ceramics, in which a two-step sintering method was applied to control grain size so as to improve the relative density of the ceramics. The studies demonstrated that it is possible to obtain high-performance BT piezoelectric ceramics by controlling both the grain size and density through optimizing the sintering conditions. Karaki et al. [55] successfully fabricated high-density BT piezoelectric ceramics with an average grain size of 1.6 mm by using hydrothermal nanoparticles through a two-step sintering method. Excellent piezoelectric performance with electromechanical coupling factor 42%, dielectric constant 5000, piezoelectric coefficients d₃₃ = 460 pC/N, and d₃₁ = 185 pC/N were obtained. The high d₃₃ of the ceramics was attributed to the high Poisson's ratio and large dielectric constants.

Ultrahigh piezoelectricity and superior electromechanical coupling properties of relaxor lead titanate (PbTiO₃, abbreviated as PT) piezoelectric single crystals were discovered. These materials exhibit a strong piezoelectric effect; 3–10-fold greater than that of conventional piezoelectric ceramics. The high piezoelectric constant and electromechanical coupling factors of relaxor-PT single crystals were found to be closely related to the engineered domain configurations [49]. Most researches on BT prepared through various processing routes have revealed promising piezoelectric performance. However, the operating temperature range of BT is limited below 120 °C due to its low Curie temperature (T_c); the critical temperature above which piezoelectric materials lose their piezoelectricity. Takenaka and Nagata [56] prepared a binary system of BaTiO₃-(Bi_{0.5}K_{0.5})TiO₃ [BKT] that exhibited an elevated T_c value of 380 °C.

In 1954, Bernard Jaffe [57] stated that the lead zirconate-lead titanate system (PZT) should have a strong piezoelectric effect near a molar compositional mix of 50/50. A noticeable feature of this material is the occurrence of a morphotropic phase boundary (MPB) (Fig. 7) that leads to composition-induced ferroelectric-to-ferroelectric phase transitions. Therefore, compositions close to the MPB boundary show excellent electromechanical properties [58]. Modified PZT compositions near the tetragonal side of the tetragonal-rhombohedral (T-R) boundary are now the most widely used piezoelectric materials. PZT shares with quartz over 90% of all piezoelectric applications [59].

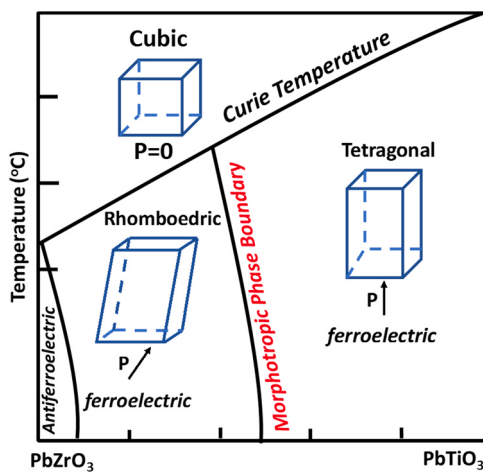


Fig. 7. Phase diagram of lead zirconate-lead titanate (PZT) compound showing crystallite structures in different regions. Piezoelectric properties of the ceramic are superior in the vicinity of the morphotropic phase boundary (MPB), at a composition of 52% lead zirconate to 48% lead titanate.

PZT ceramics have a superior piezoelectric performance with high charge coefficient (d_{33}), piezoelectric voltage coefficient (g_{33}), dielectric constant, electromechanical coupling coefficient (k_p), charge sensitivity, and energy density [60]. By tailoring zirconia (Zr) content and including doping acceptor (Mn) and donor (Nb) ions, a wide range of soft (PZT-5H), semihard (PZT-4), and hard (PZT-8) PZT materials have been developed for different applications. Zr content in PZTs determines tetragonal or rhombohedral crystal symmetry, while PZTs prepared with a composition near the MPB of these two phases displayed the highest piezoelectric property due to easy dipole reorientation [61]. Flynn and Sander [62] imposed fundamental limitations on PZT material and indicated that the mechanical stress limit is the effective constraint in typical PZT materials. They reported that a mechanical stress-limited work cycle is 330 W/cm³ at 100 kHz for PZT-5H [18].

To achieve higher piezoelectric coefficients, various compositions of PZT-based piezoelectric materials ($d_{33} = 300\text{--}1000 \text{ pC/N}$), as well as different alternate materials have been studied. A PZT-based high-performance piezoelectric generator was developed by Yi et al. [63]. Bulk PZT thick films were mounted on two sides of a flexible thin beryllium bronze substrate (50 µm) by bonding and thinning methods, and a tungsten proof mass was placed on the tip end of the cantilever beam. The thickness of top PZT layer and bottom PZT layer was reduced to 53 µm and 76 µm, respectively. The effective volume of the resultant device was 30.6 mm³. The maximum output voltage, power, and power density of 53.1 V, 0.98 mW, and 32 mW/cm³ were achieved, respectively, at an excitation force of 3.5g and frequency of 77.2 Hz. The generator was sufficient to light up twenty-one serial LEDs at resonance at 3.0g acceleration.

As is well-known, lead is a harmful component that can induce toxicity to the environment and the human body. Therefore, governments restrict its use in the manufacturing of many products. Thus, researchers have put intense effort into developing high-performance lead-free piezoelectric materials that resulted in the realization of many new piezoceramics, the most typical of which are potassium sodium niobate [(K_{0.5}Na_{0.5})NbO₃, abbreviated as KNN] and sodium bismuth titanate [(Bi_{0.5}Na_{0.5})TiO₃, abbreviated as BNT] [49,64]. Kang et al. [64] investigated the piezoelectric performance of lead-free (1 - x) BNT-xBT ceramics, sintered at 1100–1200 °C. BT has a high dielectric permittivity and high power capabilities from the equation $E = (1/2) CV^2$. Increasing both the BT content and sintering temperature improved the grain growth and densification, and consequently the piezoelectric properties. The (1 - x)BNT-xBT ceramic exhibited a piezoelectric voltage coefficient of $47.03 \times 10^{-3} \text{ Vm/N}$ at $x = 0.04$, favorably

compared to that of PZT-based ceramics. The peak piezoelectric charge coefficient of 164 pC/N and the output voltage of 8.95 V were reported at $x = 0.06$.

Shin et al. [65] studied the potentiality of using (1-x)Ba(Zr_{0.2}Ti_{0.8})O₃-x(Ba_{0.7}Ca_{0.3})TiO₃ [(1-x)BZT-xBCT] as a lead-free material in piezoelectric energy harvesting. The phase convergence region of (1-x) BZT-xBCT was studied to achieve high piezoelectric properties. The maximum piezoelectric coefficient $d_{33} = 464 \text{ pC/N}$ and the maximum energy density of 158.5 µJ/cm³ were achieved near the phase transition region between the orthorhombic and tetragonal phase. The output energy density of 158.5 µJ/cm³ was achieved which was the highest record value among lead-free ceramics. The optimal sintering temperature and optimal ceramic composition were determined to be 1475 °C and $x = 0.5$, respectively.

A lead-free non-toxic Na_xK_{1-x}NbO₃ (NKN) piezoelectric ceramic was suggested as an alternate material of the PZT, which possessed favorable piezoelectric coefficient ($d_{33} = \sim 100\text{--}400 \text{ pC/N}$) and electromechanical coupling constant ($k_p = 0.36$) [66,67]. However, both the piezoelectric coefficient and the electromechanical coupling of NKN are still much lesser than that of the PZT-based materials. The performance of the NKN-based ceramics can be enhanced by adding dopants. In the literature, ceramics of NKN with various dopants have been studied [68–74]. These NKN-based piezoelectric ceramics exhibited improved densification properties with dopants. For instance, Kim and Koh [75] used mixed oxide fabrication method to synthesize (1 - x)(Na_{0.5}K_{0.5})NbO₃-x(Bi_{0.5}Na_{0.5})TiO₃ [(1-x)NKN-xBNT] ($x = 0, 0.01, 0.03, 0.05, 0.07 \text{ mol}$) piezoelectric ceramics at various sintering temperatures between 1080 and 1160 °C [75]. A high piezoelectric coefficient of $d_{33} = 204 \text{ pC/N}$ was achieved at 0.03 mol% BNT concentration and at 1140 °C sintering temperature that yielded a maximum output power density of 24.6 nW/cm² and maximum output voltage of 10.8 V, respectively.

Aluminum nitride (AIN) thin films exhibit piezoelectric performance favorably comparable to the bulk materials. Thin films of AlN with low dielectric permittivity and high piezoelectric voltage coefficient can be prepared through a facile sputtering method. Though, its piezoelectric coefficient ($d_{33} = 3\text{--}5 \text{ pm/V}$) is still much less than PZT-based materials [66].

Most perovskite-type (ABO₃) lead-free piezoelectric materials investigated thus far exhibited relatively large piezoelectric constant. However, common drawbacks with these materials are summarized as having low Curie temperatures (T_c), difficult poling treatments, and poor relative densities. Wang et al. [76] defined the name “piezoelectric nanogenerators” after they discovered the piezoelectricity in ZnO nanowires ($d_{33} = 14\text{--}26 \text{ pm/V}$) in 2006. The advantage of using nanowires is that they can be triggered by minute physical motions and excitation frequency in a range of few Hz to multiple MHz, which is ideal for harvesting random energy in the environment such as vibrations, body motion, and gentle airflow [77]. Thus, piezoelectric nanogenerators have received significant attention from the research community. Over time, the output electric power has increased from several millivolts to several hundred volts, which is enough to drive low power devices, such as liquid crystal display (LCD) and light-emission diode (LED) [27].

Bulk inorganic materials are brittle and rigid. Therefore, several groups have fabricated them into thin films, membranes/ribbons, or nanowires to form more-flexible systems [78]. Besides, these materials have been formed into a hemisphere structure embedded in a polymer matrix, which offers flexibility and stretch-ability that broadens the range of its applications. Thus, the deformation of such structures permits the system to be stretched by up to 40% of strain, without mechanical failure [79]. In addition to the nanofibers and thin films of PZT and BT, ZnO nanowires, (1 - x)Pb(Mg_{1/3}Nb_{2/3})O₃ – xPbTiO₃ (PMN-PT) thin films, and Ba(Zr_{0.2}Ti_{0.8})O₃ – x(Ba_{0.7}Ca_{0.3})TiO₃ (BZT-BCT) nanowire/polydimethylsiloxane (PDMS) nanocomposites have been used to design flexible systems [80]. Thin films of ZnO can be

prepared through the low-temperature processes, unlike many ferroelectrics which require high-temperature processing. ZnO nanofilms can be integrated on flexible organic substrates [81]. Besides, the nanostructures are crystallographically aligned and non-ferroelectric, and therefore do not require the implementation of the poling process. ZnO has a wurtzite crystal structure, which lacks central symmetry, giving the material piezoelectric properties [82]. The final thin film is flexible and stretchable that widens the fields of its application. Nevertheless, PZT-based materials still have much higher piezoelectric coefficient and outperform ZnO materials [78,81,83].

A fully-functioning, flexible piezoelectric generator has been reported by Kim et al. [81] who grew ZnO nanorods on Au-coated woven polyester substrates. The device was completed by pressing another Au-coated polyester layer onto the surface to form a top electrode. As such, the nanorods were contacted at both their base and tip so that the piezoelectric polarization – induced by straining the rods when the cloth was bent – could be efficiently used to generate a voltage in an external circuit. An improved output was achieved by placing a 40 µm thick polyethylene (PE) spacer between the nanorods and top electrode, which produced 4 V open-circuit voltage and 0.15 µA/cm² short-circuit current density when excited by acoustic vibrations at 100 dB.

Lee et al. [84] investigated the energy harvesting capability of a hexagonal boron nitride (h-BN) nanoflakes-based flexible piezoelectric generator. h-BN nanoflakes (lateral size: 0.82 µm, thickness: 25 nm) were synthesized through a mechanochemical exfoliation process and transferred onto an electrode line-patterned plastic substrate. Mechanical bending of a single h-BN nanoflake produced alternate piezoelectric output voltage and current of 50 mV and 30 pA, respectively. Further, an h-BN nanoflakes-based flexible piezoelectric generator was fabricated that yielded a piezoelectric voltage, current, and power of 9 V, 200 nA, and 0.3 µW, respectively.

Introducing porosity into a piezoelectric material is another effective strategy to improve the piezoelectric performance. Roscow et al. [85] synthesized porous BT using polyethylene glycol as a volatile pore-forming specie. The porous composite structure changed from a 3–0 configuration (isolated pores) to a 3–3 configuration (inter-connected pores) with the increased level of porosity. A maximum energy harvesting figure of merit of 2.85 pm²/N was achieved at 60% porosity, which was three-fold higher than that of the dense samples. Such enhancement was the result of the reduced permittivity at this porosity level along with a relatively small reduction in piezoelectric coefficient d₃₃. In another study, the same research group aimed to enhance the piezoelectric energy harvesting performance of BT by forming a highly aligned porous microstructure through the freeze casting process. The freeze cast BT with 45 vol% porosity had a d₃₃ = 134.5 pC/N, which is comparable to d₃₃ = 144.5 pC/N for dense BT. Porosity considerably reduced the permittivity of BT, as such lead to an improved energy harvesting performance [86].

6.2. Organic materials

Compared to inorganic piezoelectric materials, piezoelectric polymers are naturally flexible, durable, and easy for processing, thus favorable for many applications [4,87]. The piezoelectric effect in polyvinylidene fluoride polymer (PVDF) was first observed in 1969 by Kawai [88]. Later, a copolymer of PVDF with trifluoroethylene, abbreviated as P(VDF-TrFE), was discovered. Although the magnitudes of the effects in polymers are much lower than those of ferroelectric ceramics, polymers have low permittivity and low acoustic impedance. They are available in large-area sheets (thin films), flexible, lightweight, and relatively low-cost [89]. They have large elastic compliance, and therefore can be formed on the surfaces of curved structures. PVDF has been reported to occur in α-phase, β-phase, γ-phase, and δ-phase but only the β-phase shows favorable electroactivity (piezoelectricity, ferroelectricity, and pyroelectricity), thus manifests spontaneous polarization and exhibits piezoelectricity [90,91]. High β-phase

concentration makes the PVDF highly responsive to mechanical stresses or strains. Achieving a high concentration of β-phase is aimed to obtain a resulting material highly responsive to the applied stress/strain. The beta-phase polymeric structure of PVDF is illustrated in Fig. 8. This alignment can be achieved by the poling process through mechanical stretching and subsequently applying a large static electric field at elevated temperatures [92].

Electrospun PVDF nanofibers displayed a high β-phase fraction due to the application of a high voltage during electrospinning. The electrospinning process can be effectively utilized for loaded polymers. The application of high voltages during the electrospinning process essentially leads to the alignment of the electric dipoles present in the PVDF solution, with the degree of alignment being proportional to the magnitude of the applied electric field [93]. Spin-coating is also widely used for preparing piezopolymers since it readily results in the formation of the β-phase of PVDF and copolymers [93]. Pi et al. [94] fabricated a P(VDF-TrFE) thin film-based flexible nanogenerator using the spin-coating method. The generator yielded an open-circuit voltage and short-circuit current of 7 V and 58 nA, respectively with the current density of 0.56 µA/cm².

Jin et al. [95] prepared a β-PVDF piezopolymer by a high-pressure melt crystallization process for self-powered acceleration sensors. This process allowed for obtaining high crystallinity β-phase and eliminated the need for additional poling process. A favorable linear relationship between short-circuit current and acceleration with a sensibility of 2.405 nA s² m⁻¹ was observed from 5 m/s² to 30 m/s² favorable for acceleration sensors. The generator remained stable after 10,000 repeating operation cycles under 4 Hz.

Poly(L-lactic acid) (PLLA) polymer is a green plastic derived from plants, and it is often used as an industrial raw material. The biocompatibility, flexibility, and piezoelectricity of PLLA attracted research interest in energy harvesting. Zhu et al. [96] fabricated PLLA nanofibers-based piezoelectric device for strain sensing and energy harvesting from human joint motion. Well-ordered porous PLLA nanofibers were formed on a comb-shape electrode using the electrospinning method. The direct current electric field of the electrospinning process aided polarization of the electric dipole component along the main carbon chain of PLLA nanofibers. An open-circuit voltage of 0.55 V and a short-circuit current of 230 pA were reached with a 28.9° strain deformation angle. The linear relationship between the short-circuit current and open-circuit voltage indicated that the developed piezoelectric device can be used as a strain sensor. The energy from human joint motion generated a maximum electrical power of 19.5 nW.

The low power density of piezopolymers can be overcome by introducing porosity in the material structure that reduces the effective dielectric permittivity and increases piezoelectric voltage constant. Abolhasani et al. [97] successfully formed nanopores in the electrospun P(VDF-TrFE) nanofibers through a liquid-phase de-mixing effect that was achieved by adding a certain amount of water in the polymer prior to electrospinning. Using the porous electrospun P(VDF-TrFE) nanofibers, a piezoelectric nanogenerator was fabricated that yielded as high as 500-fold greater output power at 45% porosity compared to a nonporous P(VDF-TrFE)-based nanogenerator.

6.3. Composite materials

Despite the outstanding piezoelectric performance of ceramics, their inherent brittleness limits their application in flexible devices, and despite the satisfactory flexibility of polymers, their poor piezoelectric properties restrict their use in high energy density applications. These problems can be overcome by developing composite piezoelectric materials through dispersing nanosized ceramics in a polymer matrix [98–100]. The development of nanocomposites and hybrid multiscale composites with nanosized reinforcements have made it possible to achieve simultaneous improvements in multiple structural functions and energy harvesting performance of piezoelectric generators. Various

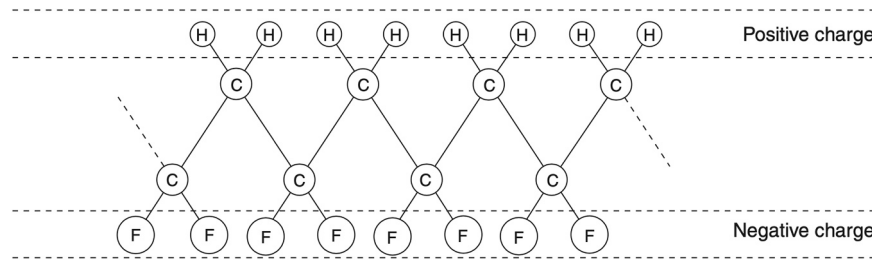


Fig. 8. Polarization of polymer chain in β -PVDF ($(\text{CH}_2\text{CF}_2)_n$). Reprinted with permission [92] Copyright 2012, Woodhead Publishing Ltd.

studies reported that the composites of PZT/PVDF exhibit comparable flexibility to native PVDF with a greater piezoelectric coefficient than native PVDF [61,101,102].

For enhancing the mechanical-to-electrical energy conversion capacity, PVDF-based piezoelectric nanogenerators have been tailored by the incorporation of the nanofillers that serve as nucleation and crystallization sites and improve β phase formation, crystal orientation, and subsequently the piezoelectric coefficient [103]. Conductive fillers, such as graphene, carbon nanotubes, carbon black, and silver, have been used to enhance nucleation and to aid the transfer of generated charges. Non-conductive fillers such as BT, KNN, ZnO, MgO, and TiO₂ have also been reported to help in nucleation and dipole alignment [11,91,93]. Among the nanofillers, BT is an extensively studied nucleating filler for PVDF-based composites owing to its high piezoelectric coefficient and biocompatibility, as well as the facile, scalable, and low-cost preparation process [104]. Many studies showed the improved piezoelectric performance of PVDF by the incorporation of BT nanofiller [104–108]. PVDF/BT-based nanocomposite thin films and fiber mats formed through solution casting and electrospinning processes exhibited enhanced dielectric constants and output power density [104,105, 108–110]. For instance, Siddiqui et al. [111] synthesized a piezoelectric nanocomposite thin film based on BT nanoparticles embedded into a highly crystalline P(VDF-TrFE). The nanocomposite generator with 40 wt% BT loading produced 9.8 V output voltage and 13.5 $\mu\text{W}/\text{cm}^2$ output power density under cyclic bending, which was comparable to those of PZT. The high piezoelectric performance of the developed nanocomposite was owing to highly crystalline P(VDF-TrFE) and its high piezoelectricity that was strengthened by BT nanoparticles [111].

Choi et al. [90] synthesized flexible piezoelectric nanocomposites with BT nanowires embedded in the PVDF matrix and studied the piezoelectric performances of the composites by varying the aspect ratio and volume fraction of the nanowire, and the duration of the poling process. It was shown that a high aspect ratio significantly increases the relative permittivity to 64. When the concentration of BT nanowires was 50 vol%, the piezoelectric coefficient was 61 pC/N, which is superior to that of composites with 50 vol% spheroid BT nanoparticles.

Siddiqui et al. [112] fabricated a nanocomposite generator based on BT nanoparticles dispersed in P(VDF-TrFE) nanofibers prepared through the electrospinning process (Fig. 9). The generator comprised of P(VDF-TrFE) electrospun nanofibers loaded with 15 wt% BT nanoparticles generated an open-circuit voltage and a short-circuit current density of 3.4 V and 0.67 $\mu\text{A}/\text{cm}^2$, respectively, with a power density of 2.28 $\mu\text{W}/\text{cm}^2$ under 20 N tapping pressure. The output voltage was observed to be stable after 10,000 tapping cycles. The generator produced an open-circuit voltage of 25 V during walking with high durability of 1000 walking steps under 600 N human body weight. The generated output power was stored in a commercial capacitor that successfully powered a strain sensor. Further, Guan et al. [16] improved the dispersion of BT nanoparticles in the P(VDF-TrFE) matrix by functionalizing BT nanoparticles with polydopamine through in situ polymerization route. A P(VDF-TrFE) nanofiber network was prepared by the electrospinning process and the functionalized BT nanoparticles were mixed in this network through ultrasonic agitation. The developed nanogenerator achieved an output voltage and current of 6 V and

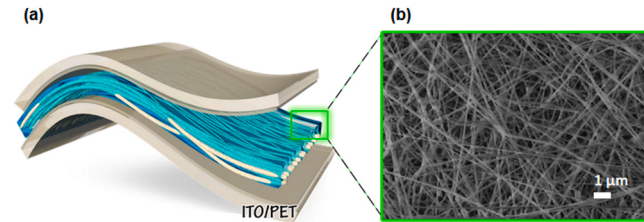


Fig. 9. (a) Schematic of the nanocomposite nanofiber generator. Top-view FE-SEM image of electrospun 35 wt% BT-P(VDF-TrFE) nanocomposite nanofibers (b) before PDMS coating. Reproduced with permission [112] Copyright 2016, Elsevier Ltd.

1.5 μA that were 4.8-fold and 2.5-fold greater than those of P(VDF-TrFE) nanogenerators, respectively. Besides, a maximum power density of 8.78 mW/m^2 was achieved. The excellent flexibility, enhanced piezoelectricity, and durability of the developed nanocomposite generator were favorable for biomechanical energy harvesting for powering wearable electronics.

Shuai et al. [113] functionalized hydroxylated BT nanoparticles with polydopamine to facilitate a uniform dispersion in PVDF scaffolds fabricated via selective laser sintering. The functionalized BT nanoparticles were uniformly distributed through the PVDF matrix, which significantly enhanced the fraction of the β phase from 46% to 59% and the output voltage by an order of 3.5-fold. As such, cell adhesion, proliferation, and differentiation were significantly enhanced. In another study, Shuai et al. [114] prepared a more complex structure by decorating polydopamine-functionalized BT nanoparticles with Ag nanoparticles through in situ growth (Fig. 10). Then, the resultant strawberry-like nanoparticles (Ag-pBT) were introduced into the PVDF scaffold fabricated by selective laser sintering. Besides inducing highly desired antibacterial property to the scaffold, Ag nanoparticles aided to enhance the polarized electric field strength on BT and to align BT nanoparticles in the direction of the applied electric field. The developed PVDF/Ag-pBT-based nanocomposite scaffold exhibited the maximum output current and voltage of 142 nA and 10 V, respectively, which were 50% and 40% greater than those of PVDF/pBT-based scaffold. In vitro cell culture tests revealed that the enhanced electric output further stimulated proliferation and differentiation of cells.

Gd₅Si₄-PVDF-based nanocomposite film was prepared by Harstad et al. [91]. The addition of 2.5–5 wt% ferromagnetic Gd₅Si₄ nanoparticles that have a high magnetic moment enhanced the crystallization of the β -phase in the PVDF film [115]. Karan et al. [91] synthesized Fe-doped reduced graphene oxide/PVDF (Fe-RGO/PVDF) nanocomposite piezoelectric material via solution casting method. Fe-RGO/PVDF nanocomposite yielded a high output voltage without applying the electric poling process. With an excitation of human finger touch, the nanocomposite film exhibited a maximum output voltage of 5.1 V and a short circuit current of 0.254 μA , which are 12-fold and 10⁵-fold greater than those of the pure PVDF, respectively.

Kang et al. [116] investigated the performance of piezoelectric composite nanofibers, which consist of NKN nanoparticles embedded

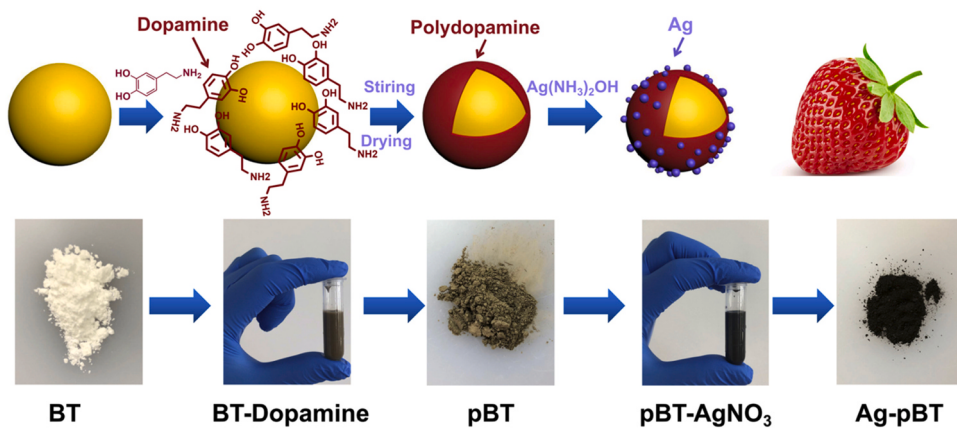


Fig. 10. Preparation process of in situ growth of Ag nanoparticles on BaTiO₃. Reproduced with permission [114] Copyright 2020, Elsevier Ltd.

along the length of P(VDF-TrFE) nanofibers. The output performance of the system was improved by the increased volume fraction of NKN nanoparticles. 0.98 V output voltage and 78 nA output current were reported at 10 vol% NKN loading.

The output performance of generators has also been reported to be effectively improved by the incorporation of conductive nanofillers such as carbon nanotubes [117–121], graphene and its derivatives [122–126], carbon black [127], and silver [128] into polymer matrix [9]. For instance, Yaqoob et al. [90] investigated the fabrication and characterization of a trilayer nanogenerator assembled by stacking a PVDF-BT layer on each side of an n-graphene layer. A maximum output voltage of 10 V was generated along with a current of 2.5 μA at an applied force of 2 N. The nanogenerator also produced 5.8 μW of instantaneous power with a 1 MΩ load resistance.

Alam and Mandal [129] studied a non-toxic cellulose-based flexible piezoelectric hybrid generator. Native cellulose microfiber and polydimethylsiloxane (PDMS) with Multi-Walled Carbon Nanotubes (MWCNTs) as conducting filler were used to prepare the hybrid generator. With the excitation of a repeating human hand punching, it produced an open circuit output voltage of ~30 V and short circuit output current of ~500 nA, corresponding to a power density ~9.0 μW/cm³ that could be sufficient to power a number of LEDs or electronic devices such as an LCD screen, calculator, or wristwatch.

Bhavanasi et al. [130] reported enhanced piezoelectric energy harvesting performance of the bilayer films of poled P(VDF-TrFE) and graphene oxide, fabricated via drop-casting of the charged dielectric film (graphene oxide) onto ferroelectric P(VDF-TrFE). The developed bilayer film exhibited a voltage output of 4 V and a power output of 4.41 μW/cm², which were superior to poled P(VDF-TrFE)-alone film that had a voltage output of 1.9 V and power output of 1.77 μW/cm². The enhanced performance of P(VDF-TrFE) with graphene oxide was attributed to multiple effects including the electrostatic contribution from graphene oxide, residual tensile stress, enhanced Young's modulus of the bilayer films, and the presence of space charge at the interface of the PVDF-TrFE film and graphene oxide film, arising from the uncompensated polarization of P(VDF-TrFE). High Young's modulus and dielectric constant of graphene oxide brought about efficient transfer of mechanical and electrical energy. The study concluded that interfacing any charged material of high dielectric constant and Young's modulus with a ferroelectric material leads to an improved energy harvesting performance.

Shi et al. [17] demonstrated that the combination of BT nanoparticles and graphene nanosheets exhibits a synergistic contribution to the piezoelectric performance of nanogenerators. A nanocomposite piezoelectric generator based on BT nanoparticles and graphene nanosheets embedded in PVDF fibers was fabricated using the electrospinning process. At 0.15 wt% graphene nanosheets and 15 wt% BT

nanoparticles loading, the open-circuit voltage and electric power of 11 V and 4.1 μW, respectively were achieved under a loading frequency of 2 Hz and 4 mm strain. The durability of the generator was demonstrated with the open-circuit voltage that remained stable after 1800 operation cycles. The generator produced a peak voltage of 112 V during a finger pressing-releasing process. This energy was sufficient to light 15 LEDs and to drive an electric watch.

In addition to P(VDF-TrFE), another copolymer of PVDF; poly(vinylidene fluoride-co-hexafluoropropylene) (PVDF-HFP) has received significant attention [11]. Ghosh et al. [103] developed a new ferroelectric nanogenerator by in situ doping of platinum nanoparticles into a PVDF-HFP matrix. The developed nanogenerator produced 18 V open-circuit output voltage and 17.7 mA short-circuit current under 4 MPa of compressive stress. The generated power could light up 55 blue LEDs, 25 green LEDs, or charge capacitors to store the generated charge. The enhanced piezoelectricity of the nanocomposite film was attributed to the enhanced piezoelectric coefficient, superior ferroelectric properties, and a high dielectric constant.

A number of metal oxide nanofillers such as MgO [131], ZnO [132, 133], NiO [134], SiO₂ [134], TiO₂ [135] have been investigated for the enhancement of the piezoelectric performance of polymers. For instance, Takhur et al. [132] observed an enhanced β-phase content of up to 84% after dispersing 0.85 vol% ZnO nanoparticles (50–150 nm) into the PVDF matrix. At 1.7 vol% nanoparticle loading, the piezoelectric coefficient increased to 50 pC/N at 50 Hz, and the dielectric constant increased to 109. Singh et al. [131] proposed a solution-processed flexible piezoelectric generator based on a nanocomposite film, consisting of MgO nanoparticles < 50 nm, embedded in P(VDF-TrFE) matrix. Compared to pure P(VDF-TrFE), the piezoelectric response of the MgO/P(VDF-TrFE) was improved by 50%, which was due to the preferred conformation of PVDF-TrFE chain, enhanced crystallinity of the P(VDF-TrFE) matrix, and uniform distribution of MgO nanoparticles through the matrix. The energy harvesting performance of MgO/P(VDF-TrFE)-based generator was superior to P(VDF-TrFE)-based generator with a two-fold greater output voltage. MgO/P(VDF-TrFE) exhibited good durability against electrical and mechanical fatigue, with the piezoelectric coefficient remained unaffected after 10,000 bending cycles.

Ren et al. [136] reported a flexible piezoelectric nanogenerator based on a composite film prepared by dispersing BiFeO₃ nanoparticles in polydimethylsiloxane (PDMS) matrix using the spin coating method. BiFeO₃ nanoparticles functioned as the power generation source while the PDMS as a flexible matrix. Under human hand impacting, the output voltage and current density of the fabricated nanogenerator were measured to be 3 V and 0.12 μA/cm², respectively, that was sufficient to instantly light a commercial light-emitting diode (LED).

A non-perovskite compound barium dititanate BaTi₂O₅ (BT2) is a

promising piezoelectric material, which exhibits strong ferroelectricity, high Curie temperature ($T_C = 430^\circ\text{C}$), and low dielectric constant ($\epsilon = \sim 100$) at room temperature [11,98]. Fu et al. [98] synthesized a BT2/PVDF-based flexible piezoelectric nanocomposite. BT2 nanorod fillers were polarized via a facile molten salt synthesis route, followed by hot pressing to control the orientation of the nanorods. Since PVDF also possesses a polar structure, the PVDF matrix was used to contribute to the piezoelectric properties of the resultant nanocomposite. A cantilever type piezoelectric generator was constructed from textured BT2/PVDF nanocomposites that exhibited an output power density of $27.4 \mu\text{W}/\text{cm}^3$ across $22 \text{ M}\Omega$ loads at an acceleration of 10 g . Besides that, the nanocomposite generator showed excellent anti-fatigue properties with the output voltage remained stable after 330,000 cycles of excitation.

Ye et al. [100] fabricated a piezoelectric generator based on P(VDF-TrFE)/boron nitride nanotubes (BNNTs) nanocomposite with a micropillar array microstructure. The strong piezoelectricity of BNNTs and the strain confinement effect of the nanocomposite micropillar array structure led to a significant enhancement of output voltage. At 0.3 wt% BNNTs loading, the output voltage and power density reached 22 V and $11.3 \mu\text{W}/\text{cm}^2$, respectively, under 0.4 MPa maximum pressure, which was 11-fold greater than that of pristine P(VDF-TrFE) film.

Vitamin B₂ was considered a potential alternative β -phase stabilizer for PVDF. Karan et al. [10] added vitamin B₂ into the PVDF matrix that stabilized β -phase PVDF by 93%. Based on this nanocomposite material, a nanogenerator was fabricated that revealed an output current of $12.2 \mu\text{A}$ and a voltage of 61.5 V . A peak power density of $9.3 \text{ mW}/\text{cm}^3$ and energy conversion efficiency of 62% was reported. This power would be sufficient to light more than 100 LEDs and could power a CD motor/mobile via capacitor charging.

A flexible generator has been reported by Kim et al. [137] who grew ZnO nanorods on Au-coated woven polyester substrates. The device was completed by pressing another Au-coated polyester layer onto the surface to form a top electrode. As such, the nanorods were contacted at both their base and tip so that the piezoelectric polarization – induced by straining the rods when the cloth was bent – could be efficiently used to generate a voltage in an external circuit. An improved output was achieved by placing a $40 \mu\text{m}$ thick polyethylene (PE) spacer between the nanorods and top electrode (Fig. 11), which produced 4 V open-circuit voltage and $0.15 \mu\text{A}/\text{cm}^2$ short-circuit current density when excited by acoustic vibrations at 100 dB .

Most polymers exhibit favorable properties such as high flexibility and acid/base resistance that enable the generators to operate under harsh conditions. However, due to low Curie temperature, their operating temperature is usually limited below 200°C . Sun et al. [8] aimed to broaden the operational temperature range of piezoelectric generators by using polyimide (PI), a highly heat-resistant polymer that can operate at a broader temperature range from -200 to 300°C . A piezoelectric nanocomposite generator was fabricated based on $0.57\text{Bi}_{0.8}\text{La}_{0.2}\text{FeO}_3\text{-}0.43\text{PbTiO}_3$ (BLF-PT) ceramic powders dispersed in the PI matrix. The BLF-PT/PI composite film was prepared via spin-coating of mechanically mixed ceramic particles and the polymer matrix. A voltage output and a current density of 110 V and $220 \text{nA}/$

cm^2 were achieved, respectively at room temperature, with the impact of a human hand. The maximum open-circuit voltage and short-circuit current were measured to be 110 V and 310nA , respectively, under 0.18 MPa pressure. The generator exhibited a voltage output of 30 V at 300°C and a high temperature stability of up to 150°C .

6.4. Bio-inspired piezoelectric materials

In addition to the widely researched ceramic, polymer, and composite piezoelectric materials, some natural biological materials such as sugar cane, cellulose, peptide, collagen fibrils, bones, hairs, etc. also show piezoelectric properties. Owing to the non-toxic, biodegradable and biocompatible nature, bio-inspired piezoelectric materials have been considered to be promising energy harvesting materials [129,138].

One of the simplest multi-cellular living organisms, sea sponge is composed of soft fibrils (e.g. spongin) and hard skeletons (e.g. spicules) in a 3D porous configuration that induces the sponge high elasticity and toughness. Zhang et al. [139] reported the performance of a sea sponge-inspired $(\text{Ba,Ca})(\text{Zr,Ti})\text{O}_3$ (BCZT) piezoceramics and elastomer matrix-based composite piezoelectric generator (Fig. 12). The 3D interconnected porous framework structure was developed based on the natural sea sponge. It was demonstrated that the mechanical and piezoelectric performance of the generator was significantly enhanced compared to those of a randomly dispersed particle-based composite generator. The output voltage, current density, and power density of 25 V , $550 \text{nA}/\text{cm}^2$ and $2.6 \text{ mW}/\text{cm}^2$, respectively, were achieved with the generator when compressed by 12%. This power density was 16-fold

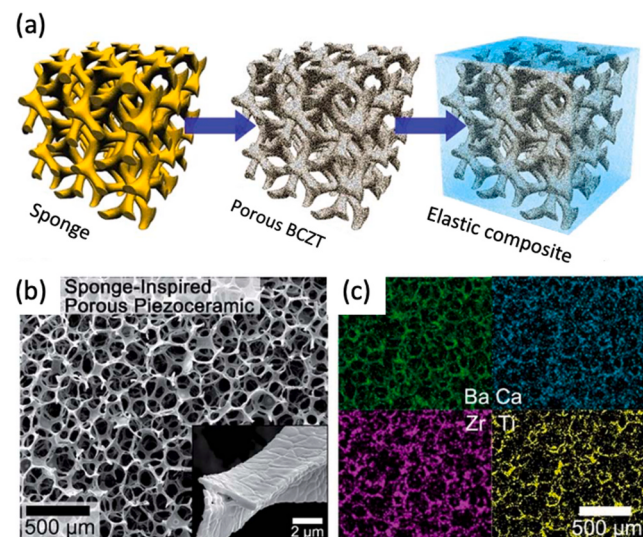


Fig. 12. (a) Schematic illustration of the fabrication process of the sea sponge-inspired 3D piezoelectric composite. (b) SEM image of the BCZT porous structure. Inset: a magnified SEM image presenting the cross-section of the porous BCZT branch. (c) EDS mapping of the BCZT porous structure. Reproduced with permission [139] Copyright 2018, Royal Society of Chemistry.

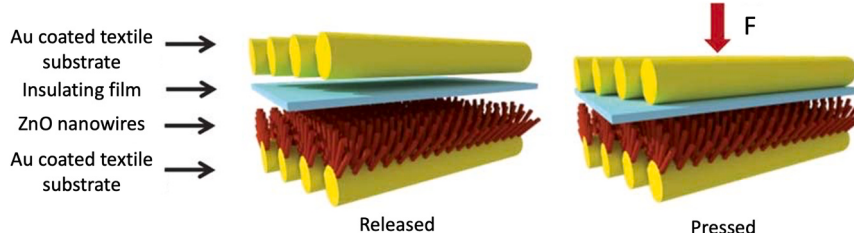


Fig. 11. Schematic of ZnO nanorod-based generator. ZnO nanorods were grown on an Au-coated polyester textile substrate with a polyethylene spacer and Au-coated polyester top electrode. Reprinted with permission [137] Copyright 2012, Royal Society of Chemistry.

greater than that of the randomly dispersed particle-based composites. A high strain–voltage efficiency was reported with an output voltage of 5 V by stretching.

Cellulose is an abundant natural polymer with favorable piezoelectric, biocompatible, and biodegradable properties. It exhibits a high piezoelectric coefficient of 26–60 pC/N [140]. Alam and Mandal [129] studied a non-toxic cellulose-based flexible piezoelectric hybrid generator. Native cellulose microfiber and polydimethylsiloxane (PDMS) with MWCNTs as conducting fillers were used to prepare the hybrid generator. With the excitation of a repeating human hand punching, it produced an open circuit output voltage of ~30 V and short circuit output current of ~500 nA, corresponding to a power density ~9.0 $\mu\text{W}/\text{cm}^3$ that could be sufficient to power a number of LEDs or electronic devices such as an LCD screen, calculator, or wristwatch.

Maiti et al. [141] used self-aligned cellulose fibrous untreated onion skin as an efficient self-poled piezoelectric material with a piezoelectric coefficient of 2.8 pC/N (Fig. 13). The fabricated generator produced an output voltage, current, instantaneous power density, and high piezoelectric energy conversion efficiency of 18 V, 166 nA, 1.7 $\mu\text{W}/\text{cm}^2$, and 61.7%, respectively. The generator was able to light 30 green LEDs under a repeated compressive stress of 34 kPa and 3.0 Hz frequency. When 6 generator units were connected in series, a maximum output voltage of 106 V was achieved which instantaneously lighted 30 green, 25 blue, or 18 red LEDs.

Zheng et al. [140] fabricated a high performance flexible piezoelectric nanogenerator based on a nanocomposite film made of cellulose nanofibers and PDMS. Cellulose nanofibers were prepared in the form of porous aerogel films through the freeze-drying process. The prepared aerogel was compressed and then coated by a PDMS layer to form the final aerogel nanocomposite film. A nanogenerator, with a size of 1 cm × 2 cm × 480 μm , was fabricated by sandwiching the prepared aerogel nanocomposite film between two thin PDMS films and two aluminum foils. An open-circuit voltage of 60.2 V, a short-circuit current of 10.1 μA , and a corresponding power density of 6.3 mW/cm^2 was achieved under the excitation by an oscillator of 10 Hz. The nanogenerator could power 19 blue LEDs and charge a capacitor to 3.7 V.

Ghosh and Mandal [142] developed a piezoelectric nanogenerator based on fish swim bladder; a waste product in fish processing (Fig. 14). It consists of highly ordered self-aligned natural collagen nanofibrils (Fig. 14d). The developed nanogenerator could convert compressive stress from a human finger (1.4 MPa) into electricity with an open circuit voltage, short circuit current, and instantaneous output power of 10 V, 51 nA, and 4.15 $\mu\text{W}/\text{cm}^2$, respectively that was sufficient to light 50 commercial blue LEDs. Karan et al. [143] investigated the potential

of using the bio-waste eggshell membrane as a piezoelectric material that exhibited a piezoelectric coefficient of 23.7 pC/N. A natural eggshell membrane-based piezoelectric nanogenerator was successfully fabricated, which yielded an output voltage of 26.4 V, 63% energy conversion efficiency, and 1.45 mA current with a peak power density of 238.2 mW/cm^2 under applied stress of 81.6 kPa. Further, an output voltage of 131 V was achieved with the series and parallel connections of five nanogenerators that lighted up 90 LEDs and generated 6 mA current, respectively. Alluri et al. [144] fabricated flexible and transparent piezoelectric aloe-vera films via the spin coating method. The prepared film had a piezoelectric coefficient d33 of 6.5 pm/V. The film was tested for harnessing the waste mechanical energy and reported to generate sufficient electric charge to act as a self-powered sensor for human finger monitoring.

A number of natural biologic systems such as eggshell membrane, fish swim bladder, and onion skin are composed of piezoelectric materials including collagen fibrils, vitamins, chitin, and so on. These natural piezoelectric materials exhibited favorable material properties such as biocompatibility, biodegradability, flexibility, and durability, which are highly desired in most applications, particularly in regenerative medicine. Besides that, generators based on bio-inspired natural materials exhibited promising piezoelectric performance. Thus, bio-inspired natural materials can help large reduction of not only biologic wastes but also toxic e-wastes generated due to the use of electrochemical batteries or lead-containing piezoelectric materials.

The output performance of generators fabricated using various piezoelectric materials are summarized in Table 1.

7. Applications of energy harvesting technologies

The advent of nano and micro-scale materials and manufacturing processes has enabled fabricating favorable materials for energy applications [145–153,154–161]. Numerous piezoelectric generators with desirable properties specific to applications such as flexibility, stretch-ability, durability, high piezoelectric performance, biocompatibility, biodegradability, etc. have been developed. As such, research groups from many diverse fields have investigated the potentiality of employing generators based on different materials to harvest ambient energy from nano to mesoscale. This section reviews the researches on the application of piezoelectric energy harvesting in various fields including transportation, structures, aerial applications, in water applications, smart systems, microfluidics, biomedical, wearable and implantable electronics, and tissue regeneration in order to present the readers the broad spectrum of applications of piezoelectric generators.

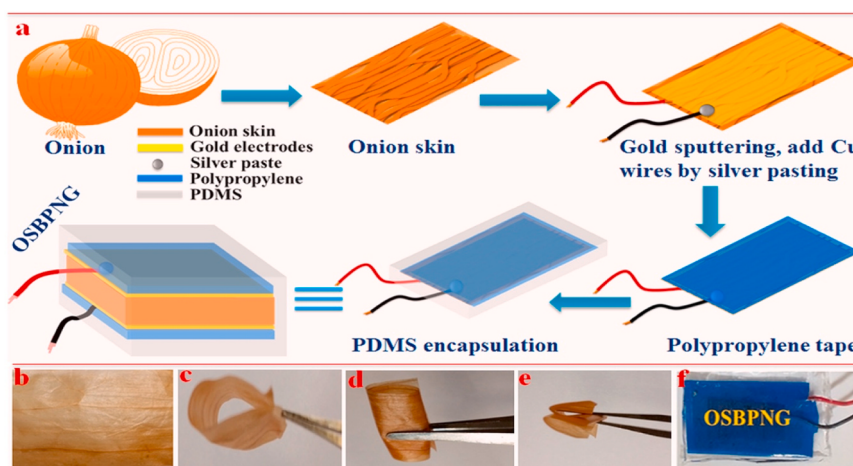


Fig. 13. (a) Schematic of fabrication of onion skin-based piezoelectric nanogenerator with a cross-section view. (b) Photograph of onion skin. The demonstration of the flexibility of onion skin under (b) bending, (d) rolling, and (e) twisting, respectively. (f) Photograph of the final generator. Reprinted with permission [141]. Copyright 2017, Elsevier Ltd.

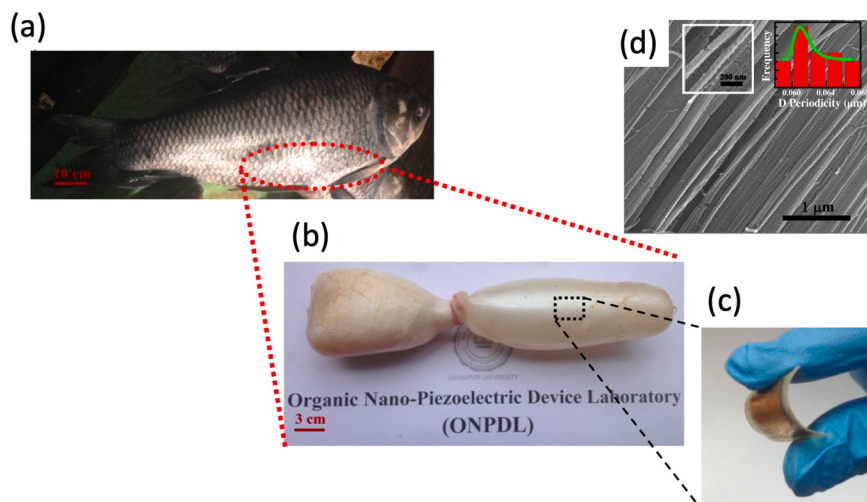


Fig. 14. Collection and preparation of the FSB for electrical characterization (a) The photograph of the sweet water (*Catla catla*) fish from where (b) the swim bladder was collected to be used in this study. (c) The flexibility of the fish swim bladder (FSB) with sputtered Au electrodes was demonstrated by a human finger. (d) FE-SEM micrograph with left inset representing a single collagen fiber to calculate the D-periodicity indicated by the histogram profile in the right inset. Reproduced with permission [142] Copyright 2016, Elsevier Ltd.

7.1. Transportation

Load mechanical energy in the road can be utilized for several purposes, such as powering traffic signal lights, monitoring the structural health of roads, self-powering vehicle weighing system, and so on. Li et al. [162] used a tracking wheel-pressure test of a beam piece to determine the piezoelectricity generating capacity of road pavement. The maximum voltage of 65.2 V was achieved. The primary wheel rolling impact produced 0.23 mJ electric energy. 0.8 kW/h electric capacity could be produced per day that would be sufficient to power traffic signal lights. The application of piezoelectric energy harvesting in asphalt has been realized in the market. An Israeli company Innowattech employs different modules with piezoelectric elements to harvest the ambient vibrational energy from asphalt [163].

7.1.1. Roadway

Harvesting energy from road traffic could be possible by using piezoelectric generators that could be a clean macro-energy source. Song et al. [164] aimed to harvest this energy by implementing piezoelectric generator modules ($30 \times 30 \times 30 \text{ cm}^3$), each contains 48 piezoelectric cantilever beams ($40 \times 60 \text{ mm}^2$) under 5 cm thick asphalt. The output power of the full-scale generator module was determined to be 736 μW . The output energy density of 4.91 Wh/m^2 was reported at 600 vehicles/h traffic rate. Under the same conditions, the generators could produce 2.95 kWh electrical power if installed along a 1 km road, along two straight lines.

Jung et al. [165] developed a PVDF-based piezoelectric generator module for energy harvesting from roadways. The study demonstrated a high-power output density, comparable to ceramic-based systems for roadway energy harvesting, by connecting sixty-unit generators in parallel. The module generated 200 mW instantaneous power output across a 40 $\text{k}\Omega$ resistor at a speed of 8 km/h and a weight of 250 kgf. Khalili et al. [166] also aimed to harvest the mechanical energy from roadways using a stack of piezoelectric generators connected in parallel. An electromechanical model was implemented, and experiments were conducted. The study achieved 95 V and 1190 V maximum voltage output, 9 mW and 1400 mW power output with a single PZT stack at a sinusoidal excitation of 1.1 kN and 11 kN, respectively, at 66 Hz frequency and 500 $\text{k}\Omega$ external resistance.

7.1.2. Rail

Gao et al. [167] proposed a $200 \text{ mm} \times 170 \text{ mm} \times 80 \text{ mm}$ piezoelectric generator to harvest rail-borne energy of wheelset/rail system, which typically has low-frequency (5–7 Hz) and low-amplitude (0.2–0.4 mm rail displacement). A hydraulic-driven system with a

loading arm at an excitation force of 140 kN was used to simulate the real wheelset/rail system. The system achieved 4.9 mW output power and 22.1 V output voltage with a 100 $\text{k}\Omega$ load impedance. The open-circuit voltage reached 24.4 V at an excitation amplitude, frequency, and acceleration of 0.2 mm, 7 Hz, and 5 g, respectively. Although the available research on energy harvesting in railway systems using piezoelectric technology is limited, a general review on energy harvesting in the railway field can be found in Ref. [168].

7.1.3. Bridge

The energy of bridge vibrations, caused by the vehicles passing through the bridge, can be converted into electrical power using vibration energy harvesters. This energy can be used for several purposes such as for lighting or for monitoring the structural health of the bridge. For instance, Karimi et al. [169] used a cantilever beam type piezoelectric generator to harvest energy from bridge vibrations. The optimal load resistance at the resonance frequency of the generator (13.5 Hz) was determined to be 200 $\text{k}\Omega$, which corresponded to a maximum power of $\sim 35 \mu\text{W}$. Wang et al. reviewed the literature on energy harvesting technologies in bridge [170]. It was concluded that in piezoelectric energy harvesting, the generated power output is usually low for individual piezoelectric transducer under one vehicle pass on the bridge. Thus, in order to generate more electric power, multiple sensor arrays under repeated traffic loading are required.

7.1.4. Speed bump

Speed bumps are constructed on the roads to control the vehicle speed to typically 5–20 km/h for traffic safety. The kinetic energy generated by the passing of a vehicle over the speed bump can be converted into electric power for wireless sensor nodes. Chen et al. [171] developed an energy harvesting system for road speed bumps, which consists of a piezoelectric impact-induced vibration cantilever energy harvester and a power management circuit. The efficiency of the system was 74% at different vehicle speeds. The total ideal energy generated by one piezoelectric cantilever from one car passing the speed bump was 1.26 mJ. It was noted that the sleep mode function of the designed circuit significantly reduced the energy losses and improved the efficiency of the speed bump energy harvester. For further reading, a review on energy harvesting from vehicular traffic over speed bumps is available in Ref. [172] by Castillo-García et al.

7.1.5. Vehicles

A small portion of only $\sim 10\text{--}16\%$ of the fuel energy is used to drive the car that overcomes the resistance from road friction and air drag while the significant portion is lost in the form of heat and mechanical

Table 1

The output performance of generators based on various piezoelectric materials.

Ref.	Material	Generator output performance
Inorganics		
Yi et al. [63]	Bulk PZT thick films	The peak output voltage is 53.1 V, power is 0.98 mW, and the power density is 32 mW/cm ³ under excitation force 3.5 g and frequency 77.2 Hz.
Kang et al. [64]	(1-x)BNT-xBT	The piezoelectric voltage coefficient is 47.03×10^{-3} Vm/N at x = 0.04.
Shin et al. [65]	[(1-x)BZT-xBCBT]	The peak piezoelectric charge coefficient is 164 pC/N and the output voltage is 8.95 V at x = 0.06.
Kim and Koh [75]	[(1-x)NKN-xBNT]	The peak piezoelectric coefficient $d_{33} = 464$ pC/N and the peak energy density is 158.5 $\mu\text{J}/\text{cm}^3$.
Kim et al. [81]	ZnO nanorods	The piezoelectric coefficient $d_{33} = 204$ pC/N at 0.03 mol% BNT. The peak output power density is 24.6 nW/cm ² and the peak output voltage is 10.8 V.
Lee et al. [84]	Hexagonal boron nitride nanoflakes (h-BN)	The open-circuit voltage is 4 V and the short-circuit current density is 0.15 $\mu\text{A}/\text{cm}^2$ under the excitation of acoustic vibrations at 100 dB.
Roscow et al. [85]	Porous BT	Single h-BN nanoflake produced alternate piezoelectric output voltage 50 mV and current 30 pA under mechanical bending. h-BN-based generator yielded a piezoelectric voltage 9 V, current 200 nA, and power 0.3 μW . The peak energy harvesting figure of merit is 2.85 pm ² /N at 60% porosity.
Organics		
Pi et al. [94]	P(VDF-TrFE) thin film	Open-circuit voltage is 7 V, short-circuit current is 58 nA, and current density is 0.56 $\mu\text{A}/\text{cm}^2$.
Zhu et al. [96]	PLLA nanofibers	Open-circuit voltage is 0.55 V and short-circuit current is 230 pA with 28.9° strain deformation angle.
Abolhasani et al. [97]	Porous P(VDF-TrFE) nanofibers	Peak electric power generated by human joint motion is 19.5 nW.
		500-fold greater output power at 45% porosity compared to nonporous P(VDF-TrFE)-based nanogenerator.
Composites		
Siddiqui et al. [111]	P(VDF-TrFE)/BT	40 wt% BT loading produced 9.8 V output voltage and 13.5 $\mu\text{W}/\text{cm}^2$ output power density under cyclic bending.
Choi et al. [90]	PVDF/(BT nanowires)	At 50 vol% BT nanowires loading, the piezoelectric coefficient is 61 pC/N.
Siddiqui et al. [112]	P(VDF-TrFE)/BT	At 15 wt% BT nanoparticles, open-circuit voltage is 3.4 V, short-circuit current density is 0.67 $\mu\text{A}/\text{cm}^2$, and power density is 2.28 $\mu\text{W}/\text{cm}^2$ under 20 N tapping pressure.
Guan et al. [16]	P(VDF-TrFE)/ (polydopamine-functionalized BT)	Open-circuit voltage of 25 V during human walking.
	PVDF/Ag-pBT	Output voltage is 6 V and current is 1.5 μA . Peak power density is 8.78 mW/m^2 .
Shuai et al. [113, 114]		Peak output current is 142 nA and voltage is 10 V, which were 50% and 40% greater than those of PVDF/pBT-based scaffold, respectively.
Karan et al. [91]	PVDF/ Fe-RGO	Output peak voltage is 5.1 V and short circuit current is 0.254 μA by human finger touch.
Kang et al. [116]	P(VDF-TrFE)/NKN	Output voltage is 0.98 V and output current is 78 nA at 10 vol% NKN loading
Yaqoob et al. [90]	PVDF-BT/n-graphene	Peak output voltage is 10 V and current is 2.5 μA under an applied force of 2 N. The nanogenerator also produced 5.8 μW of instantaneous power with a 1 Ω load resistance.
Alam and Mandal [129]	PDMS/MWCNT	Open circuit output voltage is \sim 30 V and short circuit output current is \sim 500 nA, and power density is \sim 9.0 $\mu\text{W}/\text{cm}^3$ under repeated human hand punching.
Bhavanasi et al. [130]	P(VDF-TrFE)/GO	Output voltage is 4 V and power is 4.41 $\mu\text{W}/\text{cm}^2$.
Shi et al. [17]	PVDF/BT,GO	At 0.15 wt% graphene nanosheets and 15 wt% BT nanoparticles loading, open-circuit voltage is 11 V and electric power is 4.1 μW under a loading frequency of 2 Hz and strain of 4 mm.
Ghosh et al. [103]	PVDF-HFP/Pt	The peak voltage during a finger pressing-releasing process is 112 V.
Ren et al. [136]	PDMS/ BiFeO ₃	Open-circuit output voltage is 18 V and short-circuit current is 17.7 mA under 4 MPa compressive stress.
Fu et al. [98]	BT2/PVDF	Under human hand impacting, the output voltage is 3 V and current density is 0.12 $\mu\text{A}/\text{cm}^2$.
Ye et al. [100]	P(VDF-TrFE)/BNNT	Output power density is 27.4 $\mu\text{W}/\text{cm}^3$ across 22 Ω load at 10 g acceleration.
Karan et al. [10]	PVDF/Vitamin B ₂	At 0.3 wt% BNNTs loading, the peak output voltage is 22 V and power density is 11.3 $\mu\text{W}/\text{cm}^2$ under 0.4 MPa maximum pressure.
		Output current is 12.2 μA and voltage is 61.5 V. The peak power density is 9.3 mW/cm^3 and energy conversion efficiency is 62%.
Kim et al. [137]	PE/ZnO nanorods	Open-circuit voltage is 4 V and short-circuit current density is 0.15 $\mu\text{A}/\text{cm}^2$ when excited by acoustic vibrations at 100 dB.
Sun et al. [8]	BLF-PT/PI	Output voltage is 110 V and current density is 220 nA/cm ² at room temperature, with the impact from a human hand. The peak open-circuit voltage is 110 V and short-circuit current is 310 nA under 0.18 MPa pressure.
Bio-inspired materials		
Zhang et al. [139]	Sea sponge-inspired BCZT	The output voltage is 25 V, current density is 550 nA/cm ² , and power density is 2.6 mW/cm ² when compressed by 12%.
Alam and Mandal [129]	Cellulose/PDMS/MWCNT	Open circuit output voltage is \sim 30 V, short circuit output current is \sim 500 nA, and power density is \sim 9.0 $\mu\text{W}/\text{cm}^3$ under repeating human hand punching.
Maiti et al. [141]	Onion skin	Output voltage is 18 V, current is 166 nA, instantaneous power density is 1.7 $\mu\text{W}/\text{cm}^2$, and piezoelectric energy conversion efficiency is 61.7%.
Zheng et al. [140]	Cellulose nanofibers/ PDMS	Open-circuit voltage is 60.2 V, short-circuit current is 10.1 μA , and power density is 6.3 mW/cm ³ under the excitation of oscillator at 10 Hz.
Ghosh and Mandal [142]	Fish swim bladder	Open circuit voltage is 10 V, short circuit current is 51 nA, and instantaneous output power is 4.15 $\mu\text{W}/\text{cm}^2$ under compressive stress from a human finger (1.4 MPa).
Karan et al. [143]	Eggshell membrane	Output voltage is 26.4 V, energy conversion efficiency is 63%, current is 1.45 mA, and the peak power density is 238.2 mW/cm^3 under applied stress of 81.6 kPa.

energy [173]. Absorbing mechanical energy from various parts of the vehicles such as tires, engine, and suspensions, and converting it into electrical power by using energy harvesting technologies could power various sensors that would improve the comfort, safety, and efficiency of vehicles, as well as decrease their economic and environmental costs [13].

7.1.5.1. Tire. Monitoring the pressure of tires using a wireless sensor system can significantly enhance the safety of a vehicle [174]. Energy harvesting has been proposed to exploit the structural vibration induced by the wheel rotation to power tire pressure sensors in order to eliminate the use of batteries and associated problems. Esmaeeli et al. [175] studied the design, analysis, and optimization of a rainbow-shaped piezoelectric energy harvester mounted on the inner layer of a pneumatic tire for powering a tire pressure monitoring system. The designed energy harvester generated sufficient voltage and power for the tire pressure monitoring system with high data transmission speed. The energy harvesting efficiency of one rainbow energy harvester system was calculated to be 0.69%. Bowen and Arafa summarized the literature on various energy harvesting strategies using piezoelectric, electromagnetic, electret, and triboelectric materials for self-powering of the tire pressure monitoring systems [176]. The main challenges of energy harvesting from a tire are defined as the variable and low rotational frequency of a tire, space limitation for the deployment of the harvester, and low average output power of a harvester.

7.1.5.2. Engine. Piezoelectric generators can produce electric power via harvesting torsional vibration induced by internal combustion engines. A cantilever beam structure was attached atop the surface of a rotating shaft. It generated 14 µW electrical power under 30 Nm vibrating torque. The output power can power wireless transducers such as a shaft torque transducer at a typical engine rotational speed of 2000 rpm [177].

7.1.5.3. Suspension. Xie and Wang [13] developed a mathematical model for a dual-mass piezoelectric bar generator for absorbing vibration and motion energy of a vehicle suspension system under the excitation of road roughness. The model demonstrated that output power of 738 W could be realized by a practical piezoelectric bar generator with a width and height of only 1.5 cm and 10 cm, respectively. A detailed review of vibration energy harvesting in the automotive suspension system is provided in Ref. [178].

7.2. Smart home

The location of home occupants can be used to control the electronic devices for the energy management of smart homes. To this end, a floor tile can be used to generate enough energy to wirelessly transmit the information to the electrical devices when a person steps on it. 0.72Pb_{(Zr_{0.47}Ti_{0.53})O₃}-0.28Pb[(Zn_{0.45}Ni_{0.55})_{1/3}Nb_{2/3}]O₃ + x mol% CuO (PZNxC) thick film-based self-powered floor tile was developed through the tape casting method. The piezoelectric system exhibited an output voltage and current of 42 V, 52 µA, respectively. The output voltage obtained from the footsteps of an average person (50–80 kg) on the floor tile successfully operated a wireless transmitter sensor node and the receiver switch module of the electrical device [179].

Harvesting energy from steps is an exciting topic that can be achieved by inserting piezoelectric generators either into floors or into shoes. Heel-strike energy harvesting was studied, and it was calculated that a person walking at a pace of 2 steps/s generates 67 W power that can be harvested as electrical power of 5 W using piezoelectric shoe inserts. Puscasu et al. [180] harvested step energy by using active floors. A 50 × 50 cm² energy-harvesting tile, capable of generating 2.4 mJ electrical energy per step with outstanding fatigue resistance, reaching 10 million compression cycles without decay in performance, was

developed.

7.3. Aerial applications

7.3.1. Heating, ventilation, and air conditioning (HVAC)

Petrini and Gkoumas [181] harvested flow-induced vibrations inside HVAC ducts using a piezoelectric generator in order to power a humidity sensor and a temperature sensor, as well as to wirelessly transmit the data in a building automation context. Depending on the cross-section of the aerodynamic fin, an output power in a range of 200–400 µW was achieved, which was sufficient to power a temperature sensor.

7.3.2. Wind

Flexible piezoelectric devices have been utilized to harvest wind energy. Orrego et al. [182] investigated the wind energy harvesting performance of inverted piezoelectric flags under controlled and ambient wind conditions. Inverted flag configuration offered multiple benefits such as providing sustained power generation over a wide range of wind speed, being not relied on the resonance, tunability of the resonance by adjusting the bending stiffness of the flag, and tunability to self-oscillate at any desired wind speed via adjusting its length. The peak power output of 1–5 mW/cm³ was achieved at 5–9 m/s wind speed, and 0.1–0.4 mW/cm³ was achieved at 2.5–4.5 m/s wind speeds using flags with a length of 60 mm and 100 mm, respectively.

7.4. In-water applications

Energy harvesting eel converting fluid flow energy into electrical power has been demonstrated by Taylor et al. [183]. Energy harvesting from underwater base excitation of piezoelectric beams has been investigated by Erturk et al. and Cha et al. [184,185]. Hydraulic pressure fluctuations as a source of usable energy for piezoelectric harvesting have been studied by Wang et al. and Cunefare et al. [186,187]. Further, harvesting mechanical energy from the undulations of a fishtail for developing a self-powered fish-tag has been studied by Cha et al. [188].

7.4.1. Ocean wave

Wave energy is an attractive source for energy harvesting since 70% of the Earth's surface is the ocean. It has been predicted that as high as 885 TWh electrical power can be generated from ocean wave energy [189]. Hwang et al. [190] aimed to utilize low-frequency ocean wave energy (0.5–1 Hz) by capturing the wave energy from several directions. In that regard, a piezoelectric energy harvester was designed with a cantilever structure and a magnet as the tip mass, and a tube with a metal ball moving through the tube was positioned on top. The system was tested under simulated ocean waves. The maximum output power was 68.9 µW with an impedance of 95 kΩ for a displacement of 13.2 mm. It was noted that the developed system can operate in sea-based applications involving buoys and boats.

7.4.2. Fish-tags

The migration patterns and movements of fish species can be understood by wireless communication of sensor tags implanted externally or internally in the fishes. Energy harvesting of fish swimming for self-powered fish tags is studied by Cha et al. [188]. A biomimetic fishtail was developed, which hosted two piezoelectric composites in a bimorph configuration. Both model predictions and experimental findings of the study showed that the energy from the undulating tail can power the wireless communication device.

7.4.3. Microfluidics

Wang et al. [191] developed a self-powered microfluidic sensor in order to monitor the characteristics of fluids. The fluid mechanical energy was harvested through integrating piezoelectric PVDF nanofibers with a microfluidic chip. A water droplet flowing through PVDF nanofibers, which were suspended in the fluid, could generate 1.8 V

open-circuit output voltage with the periodical deformation of the nanofibers. The impulsive output voltage signal was used for counting the droplets or bubbles in the microfluidic systems. Variation of the fluid flow condition could be monitored by the variation of the output voltage. A negative correlation between the output voltage and the input pressure and viscosity of the microfluid allowed in-situ monitoring of the fluid viscosity and pressure.

7.5. Body movement

Recently, piezoelectric energy harvesting from the movement of the human body has attracted salient attention since it can power autonomous wearable devices [192]. Kim et al. [193] developed a wearable boron nitride nanosheets-based piezoelectric generator for converting mechanical energy from human body movements into electrical energy. The generator produced a peak output voltage and output power of 22 V and 40 μ W, respectively with a power density of 106 μ W/cm³ under periodic mechanical push force of 80 kg. The generator was attached to the skin on various parts of the human body that generated output voltages of 2.5 V on the foot, 1.98 V on the elbow, 0.48 V on the neck, 0.75 V on the wrist, and 1.05 V on the knee under differential human movements.

Jung et al. [194] developed a PVDF-based curved piezoelectric generator in order to harvest low-frequency biomechanical energy from body movement for powering wearable electronics. The system generated 3.9 mW/cm² output power density that could power 476 LED bulbs. Average output power of 45 V and an average output current of 225 mA were reported at 35 Hz. Further, the developed system was integrated into a shoe-insole and to a watch strap. During running, the insole generator produced an average output voltage of 14 V and an average output current of 18 μ A while the watch generator produced an average output voltage of 22 V and an average output current of 50 μ A.

7.5.1. Walking activity

Zhou et al. [21] additively manufactured a P(VDF-TrFE)/BT nanocomposite-based flexible and stretchable kirigami-structured piezoelectric generator (Fig. 15) that can be mounted on a sock to harvest the energy from foot-stamping, and to act as a self-powered gait sensor.

Acceleration pulses caused by heel strike, acceleration from leg swing, and the compressive force acting upon the shoe due to the weight of a person are the three energy sources from walking activity that can

be harvested to generate electrical power. In order to harvest energy from these three different excitations of walking activity, Fan et al. [195] developed a piezoelectric generator, comprised of a piezoelectric cantilever beam, a crossbeam, and a ferromagnetic ball, that was mounted inside a shoe. Output voltage and power increased from 1.06 V to 3.55 V and 0.03–0.35 mW, respectively, with the variation of the walking speed from 2 km/h to 8 km/h. A detailed review of walking energy harvesting using piezoelectric materials is available in Ref. [196] by Nia et al.

7.5.2. Footfalls

Turkmen et al. [197] developed a PZT-5H piezoelectric ceramic system with a steel frame integrated into a human shoe of a weight of 90 kg. The system was able to convert 0.4% of the applied force into electrical power with an output rate of 1.43 mW. Hwang et al. [198] designed a piezoelectric tile for harvesting energy from footsteps (Fig. 16). A tile with springs and a tip mass was employed to prevent the breaking of the piezoelectric module. The developed system was tested by the impact of a free-falling steel ball, which yielded a peak output power of 55 mW.

7.6. Interactive human-machine interface

The development of an interactive human-machine interface, which transfers human intentions to the machine and collects feedback from the machine, has attracted increasing attention. The most important components of an interactive human-machine interface are flexible sensors for applications such as soft robotics and gesture recognition. Deng et al. [199] fabricated a self-powered flexible piezoelectric sensor based on cowpea-structured PVDF/ZnO nanofibers (Fig. 17), prepared via electrospinning process, for pressure sensing and for monitoring bending motions. A pressing and bending sensitivity of 0.33 V kPa⁻¹ with a response time of 16 ms, and 4.4 mV deg⁻¹ with response time of 76 ms, respectively were achieved. Besides, the PES showed good mechanical stability up to 5000 operation cycles under both working modes. A self-powered real-time gesture control system was successfully implemented by wirelessly transmitting the pulse signal from human fingers to robotic palm based on the developed piezoelectric sensor.

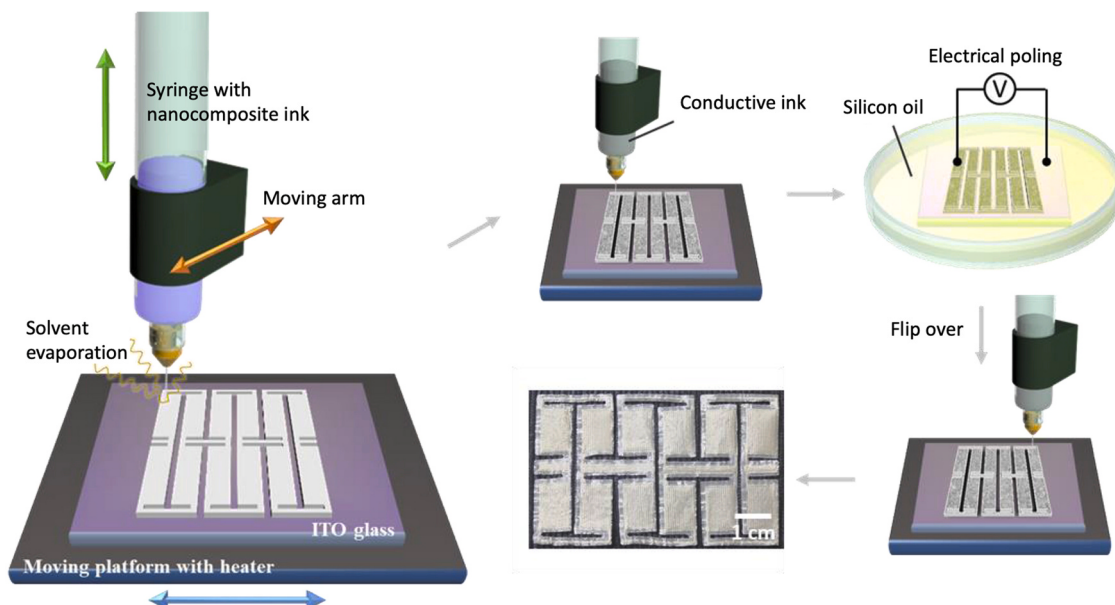


Fig. 15. Schematic illustration of the fabrication process of 3D-printed piezoelectric nanogenerator. Reprinted with permission [21] Copyright 2020, Elsevier Ltd.

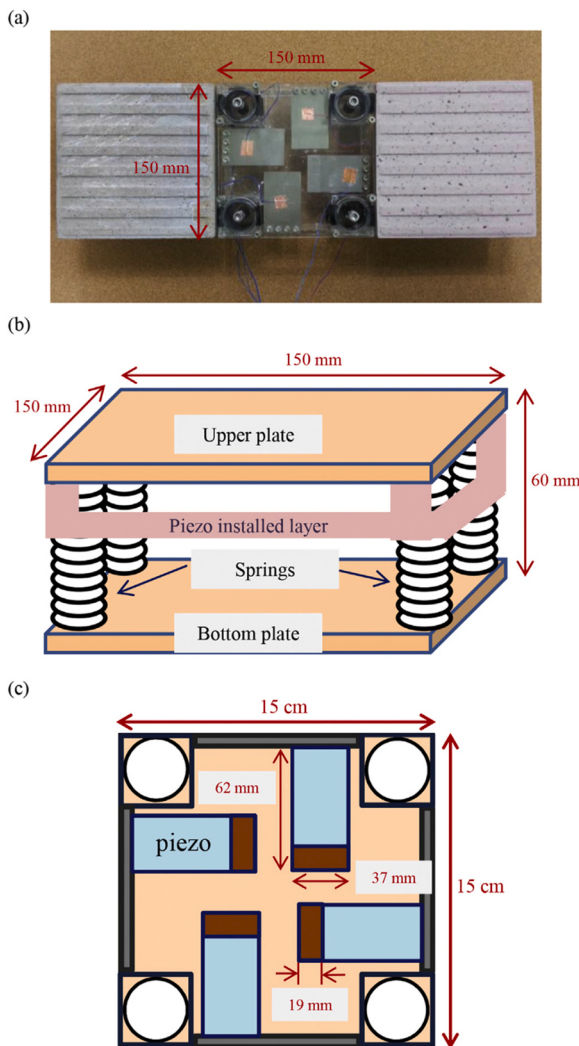


Fig. 16. Conceptual design of the piezoelectric and real tiles. (a) Real piezoelectric tile with a real tile. (b) Illustration of the piezoelectric tile. (c) Piezo-installed layer. Reprinted with permission [198] Copyright 2015, Elsevier B.V.

7.7. In vivo energy for biomedical applications

Implantable medical devices can serve as diagnostic tools and treatments to improve the quality of human life [200]. Among such devices, cardiac pacemakers, cardioverter defibrillators, cardiac monitor, bone tissue stimulators, neuronal tissue stimulators, deep brain stimulators, cochlear implants, artificial retinas, and drug delivery systems are few examples [201,202]. However, limited battery life is a major barrier in the development of these devices. Therefore, developing sustainable self-powered implantable biomedical devices is the need of the hour to reduce the physical, psychological, and financial burden on patients. In that regard, piezoelectric energy harvesting is a promising alternative to power such medical devices in order to eliminate the need of additional surgeries for the replacement of death batteries and associated morbidity and economic cost [202].

7.7.1. Cardiac energy harvesting

Cardiac pacemakers generate electrical pulses to aid the function of a heart by correcting abnormal heart rhythms caused by sick sinus syndrome or heart blockage. However, the major drawback of the pacemaker device is its short lifespan [27]. It usually lasts for 5–8 years before its battery requires a replacement by surgery that brings about increased morbidity to the patients, such as the risk of bleeding,

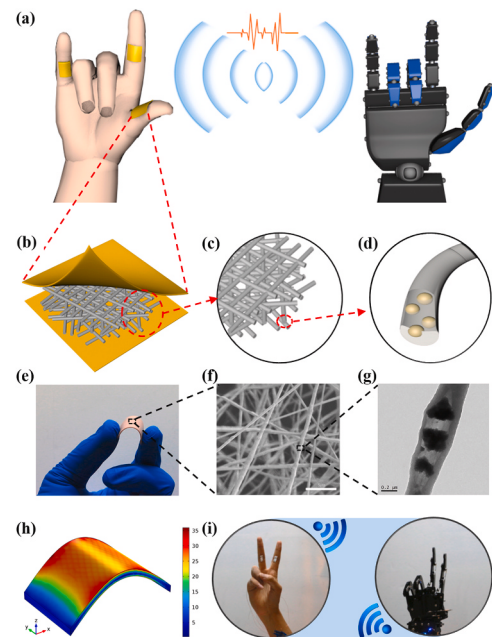


Fig. 17. The structure design of the self-powered sensor. (a) The schematic diagram of the developed smart sensor. The sketch of the device (b), NFs film (c), and a single NF (d). (e) The photograph of the fabricated sensor under bending mode. (f) The SEM image of the NFs. (g) The TEM image of a single NF. (h) The result of the FEM simulation. (i) The application of robot hand remote control is based on the PES. Reprinted with permission [199] Copyright 2018, Elsevier Ltd.

inflammation, infection, and long healing process, and additional costs on healthcare institutions [203]. Thus, cardiac energy harvesting strategies have been proposed to power the pacemakers as an alternative to the implementation of batteries [201,204–207].

Ansari and Karami [207] utilized the heartbeat vibrations to power a lead-free pacemaker using a fan-folded piezoelectric beams structure. Several piezoelectric beams stacked on each other. The size of the developed energy harvesting device was $2\text{ cm} \times 0.5\text{ cm} \times 1\text{ cm}$ that enabled operation at very high frequencies. Fan-folded geometry allowed to reduce the frequency to the desired levels and to generate more than $10\text{ }\mu\text{W}$ of power, which was sufficient to power an autonomous lead-free pacemaker.

Dong et al. [201] reported in vivo cardiac energy harvesting strategy that eliminates contact of the harvesting device with the heart and the interference with the cardiovascular function. A piezoelectric energy harvesting device based on a porous thin film with a bioinspired self-wrapping helical structure was developed to convert mechanical energy from the lead of a pacemaker or implantable cardioverter-defibrillator into electrical energy (Fig. 18). Despite the commonly used cantilever structure, the study introduced a new helical structure in order to scavenge the complex motion from a cardiac pacemaker lead. The developed harvesting device eliminates the need for additional surgeries since it integrates with the pacemaker lead and is compatible with the pacemaker lead implantation approach.

7.7.2. Cardiac sensors

Cardiac sensors are implantable medical devices capable of detecting arrhythmic symptoms with a timely response to report heartbeat conditions. With such capabilities, cardiac sensors can significantly help reducing heart diseases [200]. Piezoelectric energy harvesting has been studied for self-powered cardiac sensors [208–211]. Recently, a self-powered cardiac sensor was developed based on a flexible single-crystalline $(1-x)\text{Pb}(\text{Mg}_{1/3}\text{Nb}_{2/3})\text{O}_3 - (x)\text{Pb}(\text{Zr},\text{Ti})\text{O}_3$ (PMN-PZT) by Kim et al. [208]. The PMN-PZT-based generator

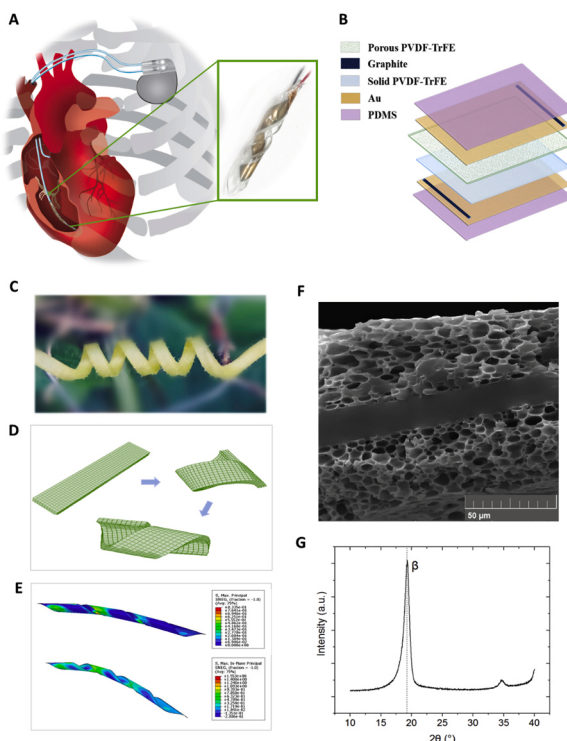


Fig. 18. Cardiac energy harvesting strategy, helical configuration, and material characterization. (A) Schematic of a helical piezoelectric energy harvester using flexible porous piezoelectric thin films. The EH device is self-wrapped around a pacemaker lead and ultimately charges the battery of the pacemaker. (B) Schematic of sandwiched PDMS/PVDF-TrFE/PDMS thin film with gold electrodes (single layer porous PVDF-TrFE EH device). (C) An example of a tendril in nature. (D) Finite element analysis for fabricating a sandwich structure of self-wrapping helical piezoelectric EH device by using the strain effect within the layers. (E) The in-plain strain distribution of the helical ribbon with different pitches by using FEA. (F) SEM image of the cross-section of sandwiched two layers of porous PVDF-TrFE thin film with the PDMS layer in between. (G) XRD spectra showing the peak associated with the crystalline β -phase at $2\theta = 19.3^\circ$. Reprinted with permission [201] Copyright 2019, Elsevier Ltd.

produced an open-circuit voltage and a short-circuit current of 17.8 V and 1.74 μ A, respectively from the contraction and relaxation of a porcine heart. The generated energy was successfully used to wirelessly switch on and off a light bulb.

7.7.3. Blood pressure monitoring

High blood pressure, so-called hypertension, is the major cause of severe diseases such as cerebrovascular disease, arteriosclerosis, retinal damage, renal failure, and heart disease [212,213]. Implanting blood pressure sensors *in vivo* could help in diagnosing these diseases and assessing the efficacy of drug treatment. Energy harvesting would allow self-powered operation of sensors to eliminate battery-related problems including current leakage, energy depletion, recharging, and limited lifetime [22,214].

Zhang et al. [202] attempted for the first time to harvest the pulsating energy of ascending aorta using a flexible and implantable piezoelectric generator based on PVDF film (Fig. 19). Ascending aorta theoretically yields the greatest output power since it exhibits the largest amplitude of deformation among all blood vessels. Experimentally, the blood circulation in ascending aorta was simulated by a latex tube of outside diameter 17 mm and a pulsating intra-aortic balloon pump. The *in vitro* pulsating energy on the latex tube was harvested by wrapping a PVDF film-based piezoelectric generator ($2.5 \text{ cm} \times 5.6 \text{ cm} \times 200 \text{ m}$) on the outer surface of the tube. Under a flow pressure of 160/80 mmHg,

the generator produced a maximum output voltage of 10.3 V and a current of 400 nA. The maximum power of 681 nW was achieved with the sampling resistor of 33 M Ω . Each pulse generated an electric charge of 7–9 nC. The generator performance was further investigated *in vivo* by wrapping it on the outer surface of the ascending aorta of a porcine model. Under the blood pressure of 160/105 mmHg, the maximum output voltage and current were measured to be 1.5 V and 300 nA, respectively. The generator had the capability to charge a 1 μ F capacitor to 1.0 V in 40 s.

Cheng et al. [215] developed a piezoelectric self-powered implantable blood pressure monitoring device based on polarized PVDF thin film that can detect hypertension status (Fig. 20). The study demonstrated the capability of the proposed system for blood pressure sensing with an instantaneous maximum power output of 2.3 μ W and 40 nW *in vitro* and *in vivo*, respectively. Favorable linearity between the peak output voltage and blood flow pressure, high sensitivity, high output power, and good stability under repeated operating cycles implied the possibility of using the developed device in clinical applications.

7.7.4. Pulse sensors

Variations in the waveform of the pulse wave carry significant information on the physiological and pathological status of the human cardiovascular system [216–218]. Therefore, real-time pulse wave monitoring is important for early prevention of diseases such as hypertension and cardiovascular disease, as well as for improving the efficacy of medical treatment [218–220].

Meng et al. [221] developed a self-powered pressure sensor based on a flexible weaving structure for noninvasive measurement of the pulse wave and blood pressure. The developed sensor had the capability to capture the mechanical change of the blood pressure in the vessel and convert it into electrical signals in the human pulse waveform. The sensor with a size of $10 \times 10 \times 1 \text{ mm}^3$ exhibited a good sensitivity of 45.7 mV Pa^{-1} with fast response time (< 5 ms), and a broad detection range (2.5–710 Pa). The durability of the sensor was demonstrated by 40,000 continuous operating cycles. No performance degradation was observed. The sensor was integrated with a system including pulse signal extraction, signal processing, and wireless transmission. As such, the measured cardiovascular parameters were communicated to the personal mobile phones. The measured results were accurate and favorably comparable to the results obtained from a commercial blood pressure measuring devices.

Park et al. [219] developed a self-powered pulse sensor for measuring radial/carotid pulse signals *in vivo*, in near-surface arteries. A high-quality PZT thin film was prepared by Sol-Gel method, then transferred onto a plastic film having a thickness of 4.8 μ m. Conformal contact between the sensor and the complex texture of the rugged skin was achieved that allowed the sensor to detect the tiniest pulse changes appearing on the surface of the epidermis. The sensitivity and response time of the sensor was measured to be 0.018 kPa^{-1} and 60 ms, respectively. Good durability was demonstrated by operating the sensor under 5000 pushing cycles. Further, the self-powered and real-time pulse monitoring system was demonstrated by a successful wireless transmission of detected arterial pressure signals to a smartphone.

7.7.5. Deep brain stimulation

The symptoms of several neurologic and psychiatric disorders such as depression, essential tremor, epilepsy, Parkinson's disease, and other movement disorders can be effectively relieved through deep brain stimulation; a neurosurgical treatment, in which specific targets in the brain is stimulated through precisely implanted electrodes by continuous electric impulses generated from a neurostimulator (also called brain stimulator or brain pacemaker) [222,223]. Neurostimulators are powered by batteries that have a limited lifetime (typically 3–5 years due to high operation power), thus require battery replacement through repetitive surgeries. Compared to cardiac pacemakers that typically operate at 2 V and 1 Hz with a pulse duration of 400 ms,

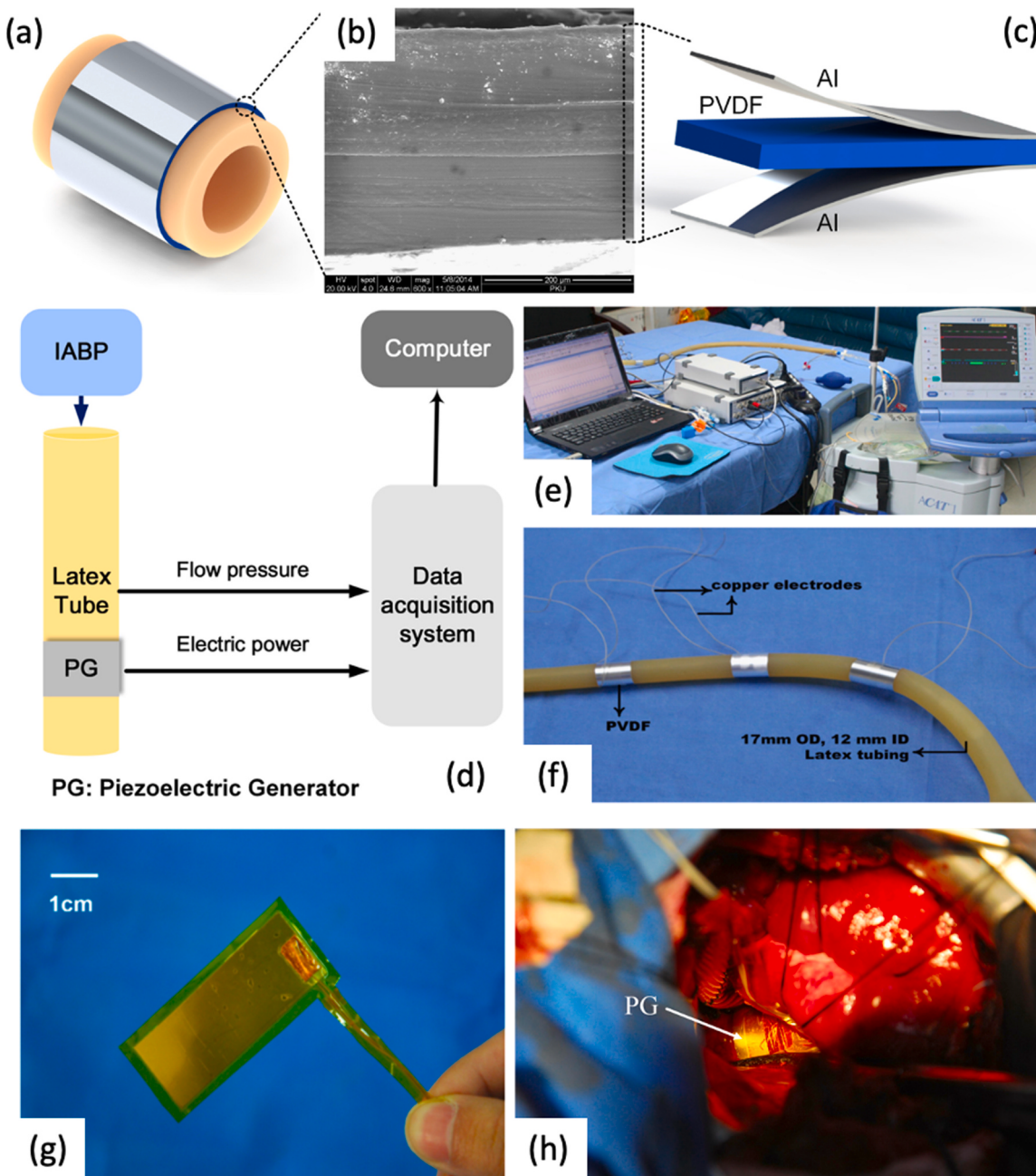


Fig. 19. (a) The schematic illustration of the piezoelectric generator (PG) wrapping around the latex tube; (b) The cross-sectional SEM images of the PG; (c) The photograph of the PG. (d) The schematic diagram of the in vitro testing system set-up; (e) Photograph of the in vitro testing system; (f) Three PGs of different size wrapping around the latex tube. (g) Photograph of the PG sealed by PI tape; (h) The implanted PG wrapping around the ascending aorta. Reprinted with permission [202]. Copyright 2015, Elsevier Ltd.

neurostimulators consume few folds higher electric power since they operate at 3–5 V and 130 Hz with pulse duration of 60 ms. Piezoelectric energy harvesting has been proposed to avoid frequent surgical procedures for the battery replacement of neurostimulators and associated problems. Fan et al. [223] suggested using energy from the human mandible to power deep brain stimulator. An experimental setup was developed to mimic the human mastication forces and analyze the energy generation performance of a piezoelectric generator mounted on the synthetic mandible. Identical output voltage waveforms were obtained by experiments and simulation by finite element analysis. Nevertheless, the power produced by the piezoelectric generator was insufficient to power a commercial brain stimulator.

Hwang et al. [222] developed a high performance flexible

piezoelectric generator based on an indium modified single-crystalline $\text{Pb}(\text{In}_{1/2}\text{Nb}_{1/2})\text{O}_3\text{-Pb}(\text{Mg}_{1/3}\text{Nb}_{2/3})\text{O}_3\text{-PbTiO}_3$ (PIMNT) thin film on a plastic substrate. The fabricated generator was utilized as a self-powered deep brain stimulator to induce forearm movements in mice. It yielded a maximum output current and voltage of 0.57 mA and 11 V, respectively from mechanical deformation and biomechanical motion. The generator energy directly stimulated a specific target area of the mice's brain to induce forearm movement. The generator successfully stimulated the M1 cortex of a living mouse that generated instantaneous bending motions of the right forelimb.

7.7.6. Tissue engineering

Electricity exists in living tissues in the form of stress-generated

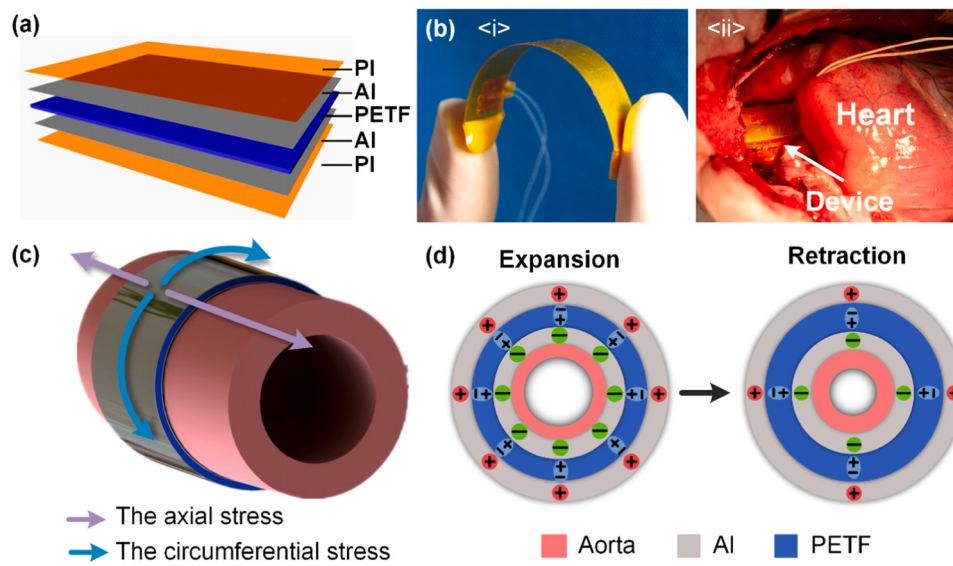


Fig. 20. (a) Exploded view of the device showing the multilayer thin-film structure. (b) Photograph of the device showing its flexibility (i) and the device wrapping on the ascending aorta of porcine (ii). (c) The circumferential stress in expanded aorta wall and the distribution of induced charge in the device. (d) The charge distributions in the device of expansion and retraction state. Reprinted with permission [215], Copyright 2016, Elsevier Ltd.

potentials, endogenous electric fields, and transmembrane potentials. The bioelectric microenvironment plays an essential role in stimulating tissue regeneration and repair [61,113,224]. The extracellular matrix is a dynamic structure that undergoes continuous remodeling. Its molecular components are subjected to several modifications. Nevertheless, the current synthetic tissue scaffolds (also named static scaffolds) remain passive and do not respond to the stimulations by external changes of the environment. Static scaffolds resist the conduction of bioelectric signals and disrupt natural signaling pathways. Stimuli-responsive scaffolds are highly desired to allow generation and transfer of bioelectric signals analogously to the native tissues to sustain proper physiological functions. Piezoelectric materials can generate electrical signals in response to the applied stress, which can be imposed even by attachment and migration of cells or body movements [225]. Thus, piezoelectric materials can be used as building blocks of active tissue engineering scaffolds that enable wireless electrical stimulation without the need for implantation of electrodes, implanting batteries, or any external electricity source [226]. Piezoelectric materials have been extensively studied for tissue repair applications, especially in neuronal and bone tissue engineering. The electric pulses stimulate neurite directional outgrowth to fill gaps in nervous tissue injuries, while charges induced by mechanical stress enhance bone formation in hard tissue injuries [44].

Attention in neural regeneration has been drawn to repairing peripheral nerve injuries through improved neural differentiation and directional outgrowth of neurites. Direct electric fields as low as 70 mV/mm have been shown to facilitate the outgrowth of the neurites of embryonic chick dorsal root ganglia toward the cathode [227]. Applying a direct electric field of 250 mV/mm or higher on Xenopus neurons resulted in more neurite-bearing cells with longer neurites directed towards the cathode and contracted neurites on the anode side (Fig. 21) [228]. Promising results are not limited to neurons; an early study on the effect of electrical stimulation on bone formation showed that implanting insulated batteries in the medullary canal of canine femora caused the substantial formation of endosteum near the cathode in a 14–21 day period [229]. Even in the absence of external electrical stimulation, implanting poled sintered piezoelectric hydroxyapatite disks in canine cortical bone resulted in the filling of a 0.2 mm gap between the negatively charged hydroxyapatite surface and the cortical bone in 14 days, while no bone formation occurred using the unpoled hydroxyapatite before day 28 [230].

7.8. Wireless power supply for implantable medical devices

In addition to electric power generation from periodical biomechanical movements such as blood circulation, cardiac/lung motions, and muscle contraction/relaxation, piezoelectric generators can also generate energy from external sources outside the human body such as inductive power transfer and acoustic energy transfer. The external power sources can provide sufficient and stable output power irrespective of the organ shape, implanted location, and body size. Jiang et al. [203] fabricated a flexible piezoelectric array based on a PZT/epoxy composite for ultrasonic energy harvesting. The developed device generated a continuous power output under ultrasonic excitation. 2.1 V_{pp} output voltage and 4.2 μA current were achieved. The generated electric power could be stored in capacitors and used to light commercial LEDs. The flexible device could maintain a favorable output performance when placed on curved surfaces. In vitro tests demonstrated that the output signals show weak attenuation performance of 15% at a mimicked implanted tissue thickness of 14 mm. These results were promising for the implementation of the developed device on wirelessly powered implantable medical devices.

8. Concluding remarks and future prospects

A comprehensive review on working mechanism, device configurations, operational modes, material developments, and applications of piezoelectric generators has been presented. Most researches employed piezoelectric generators based on unimorph and bimorph cantilever beam structure in 33 operation mode. Inorganic, organic, and composite piezoelectric materials in the nanostructure, thin-film, and stack forms have been investigated. Inorganic materials exhibit superior piezoelectric performance. However, the brittleness and toxic lead content hinder their application. Flexibility is a major requirement for the integrability of the piezoelectric generators to most applications. PVDF and its copolymers have been the most explored flexible piezopolymers. Researches have shown that the low piezoelectric performance of these polymers can be greatly enhanced through several effective strategies. One of them is to form a mesoporous structure that reduces dielectric constant and improves the piezoelectric performance of the piezopolymer. Another approach is to disperse ceramic nanofillers through the polymer matrix. This strategy attracted the utmost attention since it enabled composite generators to combine the favorable piezoelectric

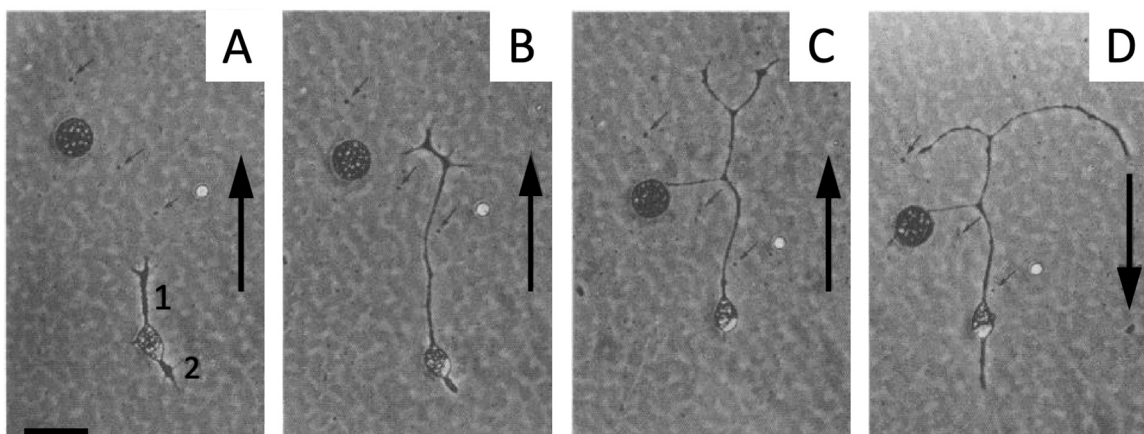


Fig. 21. Outgrowth of neurites [1 and 2 in (A)] of a bipolar neuron by means of stimulation under 500 mV/mm electric field applied in the direction of big arrows at the beginning of the electrical stimulation (A), after 2 h (B), after 4 h (C), after an additional 2 h of exposing to the electric field applied in opposite direction (D). Bar, 50 μ m [228].

performance of ceramics and the high flexibility of polymers. Surface functionalization processes are effectively applied to aid the homogeneous distribution of the nanofillers in the polymer matrix. The nanofillers aided in obtaining high crystallinity. High piezoelectricity is achieved by the homogeneous distribution and optimal concentration of nanofillers in the polymer matrix.

Besides the mostly explored inorganic and organic piezoelectric materials, many natural biologic systems such as eggshell membrane, fish swim bladder, and onion skin are composed of piezoelectric materials such as collagen fibrils, vitamins, chitin, and so on. Bio-inspired natural materials explored in the literature exhibited promising piezoelectric performance with intrinsically favorable material properties such as biocompatibility, biodegradability, flexibility, and durability. These are highly desired in most applications specifically in regenerative medicine. However, this area of research is still in its infancy and open for the exploration of many more new biomaterials. Bio-inspired natural materials can help large reduction of not only biologic wastes but also toxic e-wastes generated by the use of electrochemical batteries or lead-containing piezoelectric materials.

Developments of nano and micro-scale materials and manufacturing processes have enabled the fabrication of piezoelectric generators according to the requirements of diverse fields. The thin films of polymer and nanocomposite-based piezoelectric materials can be easily integrated into microelectromechanical systems. Besides that, nanostructured materials convert minimal mechanical strains into electric power that allows for nanoscale energy harvesting and self-powered sensing. Among nanofabrication processes, electrospinning is considered as one of the simplest and most versatile methods for fabricating nanoscale materials with diverse compositions and tailored morphologies as well as for generating remarkably long length and a wide range of fiber diameters. The networks of electrospun PVDF nanofibers exhibit a high β -phase fraction due to the high voltage applied during electrospinning. Thus, most research employed electrospun polymers for fabricating piezoelectric generators. Besides the electrospinning method, advanced manufacturing processes such as additive manufacturing by selective laser sintering and selective laser melting exhibit better control over topology, microstructure, and formation quality, thus it will attract significant attention in fabricating future piezoelectric generators, as well as active tissue scaffolds. Further, poling-assisted additive manufacturing will be a favorable alternative that can align the dipoles of the polymer molecule chains and transform the polymer from the α phase to the β phase via applying a strong electric field during printing.

In the reviewed literature, piezoelectricity has been investigated for

self-powered sensing, energy harvesting, and as a stimulator in diverse applications. Though researches revealed promising results, only a few piezoelectric products have been realized in the market while others are still in the stages of research and development. New materials have been developed to satisfy the need for specific applications. For instance, recently the development of a high-performance flexible PIMNT thin film has been demonstrated to successfully power brain stimulators, which consume much more energy than cardiac pacemakers. Besides, it is expected that new materials with enhanced properties will find applications in various fields in near future. For instance, the development of materials with high Curie temperatures will allow the deployment of piezoelectric energy harvesters in heat transfer applications that involve fluid flow. Further, it is anticipated that the attention on piezoelectric energy harvesting will continue to grow with the exploration of newer piezoelectric materials and untapped vibration sources.

Researches have demonstrated that piezoelectric generators can be effectively used for powering wearable and implantable biomedical devices as self-powered sensors for monitoring the health status of patients and as stimulators for regenerating neuronal and bone tissues. However, future researches on *in vivo* studies of piezoelectric generators are required to promote their clinical applications.

Today, the development trend of electronics is to shrink the size of devices, to reduce power consumption, and to improve device flexibility and integrate-ability. On the other hand, the development of materials and manufacturing processes enable micro and nanofabrication of piezoelectric generators with improved flexibility, integrate-ability, and output power density. Thus, it can be anticipated that in near future, piezoelectric generators will be capable of powering most wireless electronic devices.

Declaration of Competing Interest

The authors declare that they have no known competing financial interests or personal relationships that could have appeared to influence the work reported in this paper.

Acknowledgment

The authors acknowledge the support provided by Hamad Bin Khalifa University. Open Access funding provided by the Qatar National Library.

References

- [1] M. Shirvanimoghaddam, et al., Towards a green and self-powered internet of things using piezoelectric energy harvesting, *IEEE Access* 4 (2016) 1–24.
- [2] S.S. Won, H. Seo, M. Kawahara, S. Glinsek, J. Lee, Y. Kim, C.K. Jeong, A.I. Kingon, S.H. Kim, Flexible vibrational energy harvesting devices using strain-engineered perovskite piezoelectric thin films, *Nano Energy* 55 (2019) 182–192, <https://doi.org/10.1016/j.nanoen.2018.10.068>.
- [3] F. Ali, W. Raza, X. Li, H. Gul, K.H. Kim, Piezoelectric energy harvesters for biomedical applications, *Nano Energy* 57 (2019) 879–902, <https://doi.org/10.1016/j.nanoen.2019.01.012>.
- [4] H. Liu, J. Zhong, C. Lee, S.W. Lee, L. Lin, A comprehensive review on piezoelectric energy harvesting technology: materials, mechanisms, and applications, *Appl. Phys. Rev.* 5 (4) (2018), 041306, <https://doi.org/10.1063/1.5074184>.
- [5] X. Wang, Piezoelectric nanogenerators-harvesting ambient mechanical energy at the nanometer scale, *Nano Energy* 1 (1) (2012) 13–24, <https://doi.org/10.1016/j.nanoen.2011.09.001>.
- [6] C.R. Bowen, H.A. Kim, P.M. Weaver, S. Dunn, Piezoelectric and ferroelectric materials and structures for energy harvesting applications, *Energy Environ. Sci.* 7 (1) (2014) 25–44, <https://doi.org/10.1039/c3ee42454e>.
- [7] S.P. Beeby, M.J. Tudor, N.M. White, Energy harvesting vibration sources for microsystems applications, *Meas. Sci. Technol.* 17 (12) (2006) R175–R195, <https://doi.org/10.1088/0957-0233/17/12/R01>.
- [8] Y. Sun, J. Chen, X. Li, Y. Lu, S. Zhang, Z. Cheng, Flexible piezoelectric energy harvester/sensor with high voltage output over wide temperature range, *Nano Energy* 61 (2019) 337–345, <https://doi.org/10.1016/j.nanoen.2019.04.055>.
- [9] D. Hu, M. Yao, Y. Fan, C. Ma, M. Fan, M. Liu, Strategies to achieve high performance piezoelectric nanogenerators, *Nano Energy* 55 (2019) 288–304, <https://doi.org/10.1016/j.nanoen.2018.10.053>.
- [10] S.K. Karan, S. Maiti, A.K. Agrawal, A.K. Das, A. Maitra, S. Paria, A. Bera, R. Bera, L. Halder, A.K. Mishra, J.K. Kim, B.B. Khatua, Designing high energy conversion efficient bio-inspired vitamin assisted single-structured based self-powered piezoelectric/wind/acoustic multi-energy harvester with remarkable power density, *Nano Energy* 59 (2019) 169–183, <https://doi.org/10.1016/j.nanoen.2019.02.031>.
- [11] J. Yan, M. Liu, Y.G. Jeong, W. Kang, L. Li, Y. Zhao, N. Deng, B. Cheng, G. Yang, Performance enhancements in poly(vinylidene fluoride)-based piezoelectric nanogenerators for efficient energy harvesting, *Nano Energy* 56 (2019) 662–692, <https://doi.org/10.1016/j.nanoen.2018.12.010>.
- [12] D.W. Wang, J.L. Mo, X.F. Wang, H. Ouyang, Z.R. Zhou, Experimental and numerical investigations of the piezoelectric energy harvesting via friction-induced vibration, *Energy Convers. Manag.* 171 (2018) 1134–1149, <https://doi.org/10.1016/j.enconman.2018.06.052>.
- [13] X.D. Xie, Q. Wang, Energy harvesting from a vehicle suspension system, *Energy* 86 (2015) 382–395, <https://doi.org/10.1016/j.energy.2015.04.009>.
- [14] J. Chen, S.K. Oh, N. Nabulsi, H. Johnson, W. Wang, J.H. Ryou, Biocompatible and sustainable power supply for self-powered wearable and implantable electronics using III-nitride thin-film-based flexible piezoelectric generator, *Nano Energy* 57 (2019) 670–679, <https://doi.org/10.1016/j.nanoen.2018.12.080>.
- [15] C. Fei, X. Liu, B. Zhu, D. Li, X. Yang, Y. Yang, Q. Zhou, AlN piezoelectric thin films for energy harvesting and acoustic devices, *Nano Energy* 51 (2018) 146–161, <https://doi.org/10.1016/j.nanoen.2018.06.062>.
- [16] X. Guan, B. Xu, J. Gong, Hierarchically architected polydopamine modified BaTiO₃/P(VDF-TrFE) nanocomposite fiber mats for flexible piezoelectric nanogenerators and self-powered sensors, *Nano Energy* 70 (2020), 104516, <https://doi.org/10.1016/j.nanoen.2020.104516>.
- [17] K. Shi, B. Sun, X. Huang, P. Jiang, Synergistic effect of graphene nanosheet and BaTiO₃ nanoparticles on performance enhancement of electrospun PVDF nanofiber mat for flexible piezoelectric nanogenerators, *Nano Energy* 52 (2018) 153–162, <https://doi.org/10.1016/j.nanoen.2018.07.053>.
- [18] H.S. Kim, J.H. Kim, J. Kim, A review of piezoelectric energy harvesting based on vibration, *Int. J. Precis. Eng. Manuf.* 12 (6) (2011) 1129–1141, <https://doi.org/10.1007/s12541-011-0151-3>.
- [19] N. Wu, Q. Wang, X.D. Xie, Ocean wave energy harvesting with a piezoelectric coupled buoy structure, *Appl. Ocean Res.* 50 (2015) 110–118, <https://doi.org/10.1016/j.apor.2015.01.004>.
- [20] H. Madinei, H. Haddad Khodaparast, S. Adhikari, M.I. Friswell, Design of MEMS piezoelectric harvesters with electrostatically adjustable resonance frequency, *Mech. Syst. Signal Process.* 81 (2015) 360–374, <https://doi.org/10.1016/j.ymssp.2016.03.023>.
- [21] X. Zhou, K. Parida, O. Halevi, Y. Liu, J. Xiong, S. Magdassi, P.S. Lee, All 3D-printed stretchable piezoelectric nanogenerator with non-protruding kirigami structure, *Nano Energy* 72 (2020), 104676, <https://doi.org/10.1016/j.nanoen.2020.104676>.
- [22] J. Siang, M.H. Lim, M. Salman Leong, Review of vibration-based energy harvesting technology: mechanism and architectural approach, *Int. J. Energy Res.* 42 (5) (2018) 1866–1893, <https://doi.org/10.1002/er.3986>.
- [23] D.S. Snyder, Vibrating transducer power supply for use in abnormal tire condition warning systems, 1983.
- [24] D.S. Snyder, Piezoelectric reed power supply for use in abnormal tire condition warning systems, 1985.
- [25] No Title, (<http://www.perpetuum.com/rail/>), 2020.
- [26] M.A. Parvez Mahmud, N. Huda, S.H. Farjana, M. Asadnia, C. Lang, Recent advances in nanogenerator-driven self-powered implantable biomedical devices, *Adv. Energy Mater.* 8 (2) (2018), 1701210, <https://doi.org/10.1002/aenm.201701210>.
- [27] Q. Zheng, B. Shi, Z. Li, Z.L. Wang, Recent progress on piezoelectric and triboelectric energy harvesters in biomedical systems, *Adv. Sci.* 4 (7) (2017), 1700029, <https://doi.org/10.1002/advs.201700029>.
- [28] B.J. Hansen, Y. Liu, R. Yang, Z.L. Wang, Hybrid nanogenerator for concurrently harvesting biomechanical and biochemical energy, *ACS Nano* 4 (7) (2010) 3647–3652.
- [29] G. Zhu, Z.H. Lin, Q. Jing, P. Bai, C. Pan, Y. Yang, Y. Zhou, Z.L. Wang, Toward large-scale energy harvesting by a nanoparticle-enhanced triboelectric nanogenerator, *Nano Lett.* 13 (2) (2013) 847–853, <https://doi.org/10.1021/nl4001053>.
- [30] S. Priya, D.J. Inman, *Energy Harvesting Technologies*, Springer, 2009.
- [31] Z.L. Wang, W. Wu, Nanotechnology-enabled energy harvesting for self-powered micro-/nanosystems, *Angew. Chem. Int. Ed.* 51 (47) (2012) 11700–11721, <https://doi.org/10.1002/anie.201201656>.
- [32] S. Mishra, L. Unnikrishnan, S.K. Nayak, S. Mohanty, Advances in piezoelectric polymer composites for energy harvesting applications: a systematic review, *Macromol. Mater. Eng.* 304 (1) (2019), 1800463, <https://doi.org/10.1002/mame.201800463>.
- [33] B. Zaarour, L. Zhu, C. Huang, X. Jin, H. Alghafari, J. Fang, T. Lin, A review on piezoelectric fibers and nanowires for energy harvesting, *J. Ind. Text.* (2019), 152808371987019, <https://doi.org/10.1177/1528083719870197>.
- [34] V. Jella, S. Ippili, J.H. Eom, S. Pammi, J.S. Jung, V.D. Tran, V.H. Nguyen, A. Kirakosyan, S. Yun, D. Kim, M.R. Sihm, J. Choi, Y.J. Kim, H.J. Kim, S.G. Yoon, A comprehensive review of flexible piezoelectric generators based on organic-inorganic metal halide perovskites, *Nano Energy* 57 (2019) 74–93, <https://doi.org/10.1016/j.nanoen.2018.12.038>.
- [35] R.A. Surmenev, T. Orlova, R.V. Chernozem, A.A. Ivanova, A. Bartasyte, S. Mathur, M.A. Surmeneva, Hybrid lead-free polymer-based nanocomposites with improved piezoelectric response for biomedical energy-harvesting applications: a review, *Nano Energy* 62 (2019) 475–506, <https://doi.org/10.1016/j.nanoen.2019.04.090>.
- [36] S. Priya, H.C. Song, Y. Zhou, R. Varghese, A. Chopra, S.G. Kim, I. Kanno, L. Wu, D. S. Ha, J. Ryu, R.G. Polcawich, A review on piezoelectric energy harvesting: materials, methods, and circuits, *Energy Harvest. Syst.* 4 (1) (2019) 3–39, <https://doi.org/10.1515/ehs-2016-0028>.
- [37] M. Hamlehdar, A. Kasaeian, M.R. Safaei, Energy harvesting from fluid flow using piezoelectrics: a critical review, *Renew. Energy* 143 (2019) 1826–1838, <https://doi.org/10.1016/j.renene.2019.05.078>.
- [38] M. Gholikhani, H. Roshani, S. Dessouky, A.T. Papagiannakis, A critical review of roadway energy harvesting technologies, *Appl. Energy* 261 (2020), 114388, <https://doi.org/10.1016/j.apenergy.2019.114388>.
- [39] J. Wang, L. Geng, L. Ding, H. Zhu, D. Yurchenko, The state-of-the-art review on energy harvesting from flow-induced vibrations, *Appl. Energy* 267 (2020), 114902, <https://doi.org/10.1016/j.apenergy.2020.114902>.
- [40] J. Chen, Q. Qiu, Y. Han, D. Lau, Piezoelectric materials for sustainable building structures: fundamentals and applications, *Renew. Sustain. Energy Rev.* 101 (2019) 14–25, <https://doi.org/10.1016/j.rser.2018.09.038>.
- [41] M.R. Sarker, S. Julai, M.F.M. Sabri, S.M. Said, M.M. Islam, M. Tahir, Review of piezoelectric energy harvesting system and application of optimization techniques to enhance the performance of the harvesting system, *Sens. Actuators A Phys.* 300 (2019), 111634, <https://doi.org/10.1016/j.sna.2019.111634>.
- [42] Q. Lu, L. Liu, F. Scarpa, J. Leng, Y. Liu, A novel composite multi-layer piezoelectric energy harvester, *Compos. Struct.* 201 (2018) 121–130, <https://doi.org/10.1016/j.compstruct.2018.06.024>.
- [43] S. Beeby, N. White, Energy harvesting for autonomous systems, 2010.
- [44] A.H. Rajabi, M. Jaffé, T.L. Arinze, Piezoelectric materials for tissue regeneration: a review, *Acta Biomater.* 24 (2015) 12–23, <https://doi.org/10.1016/j.actbio.2015.07.010>.
- [45] A. Jain, K.J. Prashanth, A.K. Sharma, A. Jain, R. P.n, Dielectric and piezoelectric properties of PVDF/PZT composites: a review, *Polym. Eng. Sci.* 55 (7) (2015) 1589–1616, <https://doi.org/10.1002/pen.24088>.
- [46] Y. Sugawara, K. Onitsuka, S. Yoshikawa, Q. Xu, R.E. Newnham, K. Uchino, Metal-ceramic composite actuators, *J. Am. Ceram. Soc.* 75 (4) (1992) 996–998, <https://doi.org/10.1111/j.1151-2916.1992.tb04172.x>.
- [47] L. Li, J. Xu, J. Liu, F. Gao, Recent progress on piezoelectric energy harvesting: structures and materials, *Adv. Compos. Hybrid Mater.* 1 (3) (2018) 478–505, <https://doi.org/10.1007/s42114-018-0046-1>.
- [48] D. Arnold, W. Kinsel, W.W. Clark, C. Mo, Exploration of new cymbal design in energy harvesting, in: SPIE Proceedings, 2011, 79770T. doi: 10.1117/12.880614.
- [49] J. Hao, W. Li, J. Zhai, H. Chen, Progress in high-strain perovskite piezoelectric ceramics, *Mater. Sci. Eng. R Rep.* 135 (2019) 1–57, <https://doi.org/10.1016/j.mser.2018.08.001>.
- [50] D.F.K. Hennings, C. Metzmacher, B.S. Schreinemacher, Defect chemistry and microstructure of hydrothermal barium titanate, *J. Am. Ceram. Soc.* 84 (1) (2001) 179–182, <https://doi.org/10.1111/j.1151-2916.2001.tb00627.x>.
- [51] S. Wada, K. Yako, H. Kakemoto, T. Tsurumi, T. Kiguchi, Enhanced piezoelectric properties of barium titanate single crystals with different engineered-domain sizes, *J. Appl. Phys.* 98 (1) (2005), 014109, <https://doi.org/10.1063/1.1957130>.
- [52] H. Takahashi, Y. Numamoto, J. Tani, K. Matsuta, J. Qiu, S. Tsurekawa, Lead-free barium titanate ceramics with large piezoelectric constant fabricated by microwave sintering, *Jpn. J. Appl. Phys.* 45 (1) (2006) L30–L32, <https://doi.org/10.1143/JJAP.45.L30>.

- [53] A. Polotai, K. Breece, E. Dickey, C. Randall, A. Ragulya, A novel approach to sintering nanocrystalline barium titanate ceramics, *J. Am. Ceram. Soc.* 88 (11) (2005) 3008–3012, <https://doi.org/10.1111/j.1551-2916.2005.00552.x>.
- [54] X.-H. Wang, X.Y. Deng, H.L. Bai, H. Zhou, W.G. Qu, L.T. Li, I.W. Chen, Two-step sintering of ceramics with constant grain-size, II: BaTiO₃ and Ni-Cu-Zn ferrite, *J. Am. Ceram. Soc.* 89 (2) (2006) 438–443, <https://doi.org/10.1111/j.1551-2916.2005.00728.x>.
- [55] T. Karaki, K. Yan, T. Miyamoto, M. Adachi, Lead-free piezoelectric ceramics with large dielectric and piezoelectric constants manufactured from BaTiO₃ nanopowder, *Jpn. J. Appl. Phys. Part 2 Lett.* 46 (4–7) (2007) 97–99, <https://doi.org/10.1143/JJAP.46.L97>.
- [56] T. Takenaka, H. Nagata, Current status and prospects of lead-free piezoelectric ceramics, *J. Eur. Ceram. Soc.* 25 (12) (2005) 2693–2700, <https://doi.org/10.1016/j.jeurceramsoc.2005.03.125>.
- [57] B. Jaffe, R.S. Roth, S. Marzullo, Piezoelectric properties of lead zirconate-lead titanate solid-solution ceramics, *J. Appl. Phys.* 25 (6) (1954) 809–810, <https://doi.org/10.1063/1.1721741>.
- [58] M.D. Maeder, D. Damjanovic, N. Setter, Lead free piezoelectric materials, *J. Electroceram.* 13 (1–3) (2004) 385–392, <https://doi.org/10.1007/s10832-004-5130-y>.
- [59] D. Berlingcourt, Piezoelectric ceramic compositional development, *J. Acoust. Soc. Am.* 91 (5) (1992) 3034–3040.
- [60] D.J. Shin, S.J. Jeong, C.E. Seo, K.H. Cho, J.H. Koh, Multi-layered piezoelectric energy harvesters based on PZT ceramic actuators, *Ceram. Int.* 41 (S1) (2015) S686–S690, <https://doi.org/10.1016/j.ceramint.2015.03.180>.
- [61] K. Kapat, Q.T.H. Shubhra, M. Zhou, S. Leeuwenburgh, Piezoelectric nanobiomaterials for biomedicine and tissue regeneration, *Adv. Funct. Mater.* 1909045 (2020), 1909045, <https://doi.org/10.1002/adfm.201909045>.
- [62] A.M. Flynn, S.R. Sanders, Fundamental limits on energy transfer and circuit considerations for piezoelectric transformers, *IEEE Trans. Power Electron.* 17 (1) (2002) 8–14, <https://doi.org/10.1109/63.988662>.
- [63] Z. Yi, B. Yang, G. Li, J. Liu, X. Chen, X. Wang, C. Yang, High performance bimorph piezoelectric MEMS harvester via bulk PZT thick films on thin beryllium-bronze substrate, *Appl. Phys. Lett.* 111 (1) (2017), 013902, <https://doi.org/10.1063/1.4991368>.
- [64] W.S. Kang, J.H. Koh, (1-x)Bi0.5Na0.5TiO3-xBaTiO3 lead-free piezoelectric ceramics for energy-harvesting applications, *J. Eur. Ceram. Soc.* 35 (7) (2015) 2057–2064, <https://doi.org/10.1016/j.jeurceramsoc.2014.12.036>.
- [65] D.J. Shin, J. Kim, J.H. Koh, Piezoelectric properties of (1-x)BZT-xBCT system for energy harvesting applications, *J. Eur. Ceram. Soc.* 38 (13) (2018) 4395–4403, <https://doi.org/10.1016/j.jeurceramsoc.2018.05.022>.
- [66] A. Khan, Z. Abas, H. Soo Kim, I.K. Oh, Piezoelectric thin films: an integrated review of transducers and energy harvesting, *Smart Mater. Struct.* 25 (5) (2016), 053002, <https://doi.org/10.1088/0964-1726/25/5/053002>.
- [67] B. Ponraj, R. Bhimireddi, K.B.R. Varma, Effect of nano- and micron-sized K0.5Na0.5NbO3 fillers on the dielectric and piezoelectric properties of PVDF composites, *J. Adv. Ceram.* 5 (4) (2016) 308–320, <https://doi.org/10.1007/s40145-016-0204-2>.
- [68] Y. Wang, J. Wu, D. Xiao, J. Zhu, Y. Jin, J. Zhu, P. Yu, L. Wu, X. Li, Microstructure, dielectric, and piezoelectric properties of (Li, Ag, Ta) modified (K0.50Na0.50) NbO3 lead-free ceramics with high Curie temperature, *J. Appl. Phys.* 102 (5) (2007), 054101, <https://doi.org/10.1063/1.2773687>.
- [69] Y. Guo, K. Kakimoto, H. Ohsato, (Na0.5K0.5)NbO3-LiTaO3 lead-free piezoelectric ceramics, *Mater. Lett.* 59 (2–3) (2005) 241–244, <https://doi.org/10.1016/j.matlet.2004.07.057>.
- [70] S. Zhang, R. Xia, T.R. Shrout, G. Zang, J. Wang, Piezoelectric properties in perovskite 0.948(K0.5Na0.5)NbO3–0.052Li₂SiO₃ lead-free ceramics, *J. Appl. Phys.* 100 (10) (2006), 104108, <https://doi.org/10.1063/1.2382348>.
- [71] H. Du, F. Tang, D. Liu, D. Zhu, W. Zhou, S. Qu, The microstructure and ferroelectric properties of (K0.5Na0.5)NbO3–LiNbO3 lead-free piezoelectric ceramics, *Mater. Sci. Eng. B* 136 (2–3) (2007) 165–169, <https://doi.org/10.1016/j.mseb.2006.09.031>.
- [72] Y. Guo, K. Kakimoto, H. Ohsato, Dielectric and piezoelectric properties of lead-free (Na0.5K0.5)NbO3–SrTiO₃ ceramics, *Solid State Commun.* 129 (5) (2004) 279–284, <https://doi.org/10.1016/j.ssc.2003.10.026>.
- [73] S.-T. Zhang, A.B. Kounga, E. Aulbach, T. Granzow, W. Jo, H.J. Kleebe, J. Rödel, Lead-free piezoceramics with giant strain in the system Bi0.5Na0.5TiO₃–BaTiO₃–K0.5Na0.5NbO₃. I. Structure and room temperature properties, *J. Appl. Phys.* 103 (3) (2008), 034107, <https://doi.org/10.1063/1.2838472>.
- [74] R. Wang, R.X. Xie, K. Hanada, K. Matsusaki, H. Kawanaka, H. Bando, T. Sekiya, M. Itoh, Enhanced piezoelectricity around the tetragonal/orthorhombic morphotropic phase boundary in (Na,K)NbO₃–AlTiO₃ solid solutions, *J. Electroceram.* 21 (1–4) (2008) 263–266, <https://doi.org/10.1007/s10832-007-9136-0>.
- [75] J. Kim, J.H. Koh, (Na,K)NbO₃–(Bi,Na)TiO₃ piezoelectric ceramics for energy-harvesting applications, *J. Eur. Ceram. Soc.* 35 (14) (2015) 3819–3825, <https://doi.org/10.1016/j.jeurceramsoc.2015.07.008>.
- [76] X. Wang, J. Song, J. Liu, Z.L. Wang, Direct-current nanogenerator driven by ultrasonic waves, *Science* 316 (5821) (2007) 102–105, <https://doi.org/10.1126/science.1139366>.
- [77] Z.L. Wang, G. Zhu, Y. Yang, S. Wang, C. Pan, Progress in nanogenerators for portable electronics, *Mater. Today* 15 (12) (2012) 532–543, [https://doi.org/10.1016/S1369-7021\(13\)70011-7](https://doi.org/10.1016/S1369-7021(13)70011-7).
- [78] W. Wu, S. Bai, M. Yuan, Y. Qin, Z.L. Wang, T. Jing, Lead zirconate titanate nanowire textile nanogenerator for wearable energy-harvesting and self-powered devices, *ACS Nano* 6 (7) (2012) 6231–6235, <https://doi.org/10.1021/nm3016585>.
- [79] J. Chun, N.R. Kang, J.Y. Kim, M.S. Noh, C.Y. Kang, D. Choi, S.W. Kim, Z. Lin Wang, J. Min Baik, Highly anisotropic power generation in piezoelectric hemispheres composed stretchable composite film for self-powered motion sensor, *Nano Energy* 11 (2015) 1–10, <https://doi.org/10.1016/j.nanoen.2014.10.010>.
- [80] C. Dagdeviren, Z. Li, Z.L. Wang, Energy harvesting from the animal/human body for self-powered electronics, *Annu. Rev. Biomed. Eng.* 19 (1) (2017) 85–108, <https://doi.org/10.1146/annurev-bioeng-071516-044517>.
- [81] J. Briscoe, S. Dunn, Piezoelectric nanogenerators - a review of nanostructured piezoelectric energy harvesters, *Nano Energy* 14 (2014) 15–29, <https://doi.org/10.1016/j.nanoen.2014.11.059>.
- [82] L. Dong, C. Jin, A.B. Closson, I. Trase, H.C. Richards, Z. Chen, J. Zhang, Cardiac energy harvesting and sensing based on piezoelectric and triboelectric designs, *Nano Energy* 76 (2020), 105076, <https://doi.org/10.1016/j.nanoen.2020.105076>.
- [83] M.G. Kang, W.S. Jung, C.Y. Kang, S.J. Yoon, Recent progress on PZT based piezoelectric energy harvesting technologies, *Actuators* 5 (1) (2016), <https://doi.org/10.3390/act5010005>.
- [84] G.J. Lee, M.K. Lee, J.J. Park, D.Y. Hyeon, C.K. Jeong, K. Il Park, Piezoelectric energy harvesting from two-dimensional boron nitride nanoflakes, *ACS Appl. Mater. Interfaces* 11 (41) (2019) 37920–37926, <https://doi.org/10.1021/acsm.nano.9b12187>.
- [85] J.I. Roscow, Y. Zhang, M.J. Krašný, R.W.C. Lewis, J. Taylor, C.R. Bowen, Freeze cast porous barium titanate for enhanced piezoelectric energy harvesting, *J. Phys. D. Appl. Phys.* 51 (22) (2018), 225301, <https://doi.org/10.1088/1361-6463/aabc81>.
- [86] J.I. Roscow, J. Taylor, C.R. Bowen, Manufacture and characterization of porous ferroelectrics for piezoelectric energy harvesting applications, *Ferroelectrics* 498 (1) (2016) 40–46, <https://doi.org/10.1080/00150193.2016.1169154>.
- [87] S.R. Anton, H.A. Sodano, A review of power harvesting using piezoelectric materials (2003–2006), *Smart Mater. Struct.* 16 (3) (2007) R1–R21, <https://doi.org/10.1088/0964-1726/16/3/R01>.
- [88] H. Kawai, The piezoelectricity of poly (vinylidene fluoride), *Jpn. J. Appl. Phys.* 8 (7) (1969) 975–976.
- [89] S.B. Lang, S. Muensit, Review of some lesser-known applications of piezoelectric and pyroelectric polymers, *Appl. Phys. A Mater. Sci. Process.* 85 (2) (2006) 125–134, <https://doi.org/10.1007/s00339-006-3688-8>.
- [90] F. Narita, M. Fox, A review on piezoelectric, magnetostrictive, and magnetoelectric materials and device technologies for energy harvesting applications, *Adv. Eng. Mater.* 20 (5) (2018), 1700743, <https://doi.org/10.1002/adem.201700743>.
- [91] S.K. Karan, D. Mandal, B.B. Khatua, Self-powered flexible Fe-doped RGO/PVDF nanocomposite: an excellent material for a piezoelectric energy harvester, *Nanoscale* 7 (24) (2015) 10655–10666, <https://doi.org/10.1039/c5nr02067k>.
- [92] M.E. Kiziroglou, E.M. Yeatman, *Materials and Techniques for Energy Harvesting*, Woodhead Publishing Limited, 2012.
- [93] R.A. Surnevet, T. Orlova, R.V. Chernozem, A.A. Ivanova, A. Bartasyte, S. Mathur, M.A. Surneneva, Hybrid lead-free polymer-based nanocomposites with improved piezoelectric response for biomedical energy-harvesting applications: a review, *Nano Energy* 62 (2019) 475–506, <https://doi.org/10.1016/j.nanoen.2019.04.090>.
- [94] Z. Pi, J. Zhang, C. Wen, Z. bin Zhang, D. Wu, Flexible piezoelectric nanogenerator made of poly(vinylidenefluoride-co-trifluoroethylene) (PVDF-TrFE) thin film, *Nano Energy* 7 (2014) 33–41, <https://doi.org/10.1016/j.nanoen.2014.04.016>.
- [95] L. Jin, S. Ma, W. Deng, C. Yan, T. Yang, X. Chu, G. Tian, D. Xiong, J. Lu, W. Yang, Polarization-free high-crystallinity β-PVDF piezoelectric nanogenerator toward self-powered 3D acceleration sensor, *Nano Energy* 50 (2018) 632–638, <https://doi.org/10.1016/j.nanoen.2018.05.068>.
- [96] J. Zhu, L. Jia, R. Huang, Electrospinning poly(l-lactic acid) piezoelectric ordered porous nanofibers for strain sensing and energy harvesting, *J. Mater. Sci. Mater. Electron.* 28 (16) (2017) 12080–12085, <https://doi.org/10.1007/s10854-017-7020-5>.
- [97] M.M. Abolhasani, M. Naebe, K. Shirvanimoghaddam, H. Fashandi, H. Khayyam, M. Joordens, A. Piperts, S. Anwar, R. Berger, G. Floudas, J. Michels, K. Asadi, Thermodynamic approach to tailor porosity in piezoelectric polymer fibers for application in nanogenerators, *Nano Energy* 62 (2019) 594–600, <https://doi.org/10.1016/j.nanoen.2019.05.044>.
- [98] J. Fu, Y. Hou, X. Gao, M. Zheng, M. Zhu, Highly durable piezoelectric energy harvester based on a PVDF flexible nanocomposite filled with oriented BaTiO₃ nanorods with high power density, *Nano Energy* 52 (2018) 391–401, <https://doi.org/10.1016/j.nanoen.2018.08.006>.
- [99] L. Yang, et al., Preparationand characterization of a novel piezoelectric nanogenerator based on solubleand meltable copolyimide for harvesting mechanical energy, *Nano Energy* 67 (2020), 104220, <https://doi.org/10.1016/j.nanoen.2019.104220>.
- [100] S. Ye, C. Cheng, X. Chen, J. Shao, J. Zhang, H. Hu, H. Tian, X. Li, L. Ma, W. Jia, High-performance piezoelectric nanogenerator based on microstructured PVDF-TrFE/BNNt composite for energy harvesting and radiation protection in space, *Nano Energy* 60 (2019) 701–714, <https://doi.org/10.1016/j.nanoen.2019.03.096>.
- [101] W.B. Harrison, Flexible piezoelectric organic composites, in: Proceedings of the Workshop on Sonar Transducer Materials, 1976, 257–268.

- [102] W.A. Smith, The role of piezocomposites in ultrasonic transducers, in: Proceedings IEEE Ultrasonics Symposium, 755–766, doi: [10.1109/ULTSYM.1989.67088](https://doi.org/10.1109/ULTSYM.1989.67088).
- [103] S.K. Ghosh, T.K. Sinha, B. Mahanty, D. Mandal, Self-poled efficient flexible ‘ferroelectric’ nanogenerator: a new class of piezoelectric energy harvester, *Energy Technol.* 3 (12) (2015) 1190–1197, <https://doi.org/10.1002/ente.201500167>.
- [104] C.K. Jeong, C. Baek, A.I. Kingon, K.-I. Park, S.-H. Kim, Lead-free perovskite nanowire-employed piezopolymer for highly efficient flexible nanocomposite energy harvester, *Small* 14 (19) (2018), 1704022, <https://doi.org/10.1002/smll.201704022>.
- [105] C. Mota, M. Labardi, L. Trombi, L. Astolfi, M. D’Acunto, D. Puppi, G. Gallone, F. Chiellini, S. Berrettini, L. Bruschini, S. Danti, Design, fabrication and characterization of composite piezoelectric ultrafine fibers for cochlear stimulation, *Mater. Des.* 122 (2017) 206–219, <https://doi.org/10.1016/j.matdes.2017.03.013>.
- [106] S. Siddiqui, D.I. Kim, L.T. Duy, M.T. Nguyen, S. Muhammad, W.S. Yoon, N.E. Lee, High-performance flexible lead-free nanocomposite piezoelectric nanogenerator for biomechanical energy harvesting and storage, *Nano Energy* 15 (2015) 177–185, <https://doi.org/10.1016/j.nanoen.2015.04.030>.
- [107] S.-H. Shin, Y.-H. Kim, M.H. Lee, J.-Y. Jung, J. Nah, Hemispherically aggregated BaTiO₃ nanoparticle composite thin film for high-performance flexible piezoelectric nanogenerator, *ACS Nano* 8 (3) (2014) 2766–2773, <https://doi.org/10.1021/nn406481k>.
- [108] N.R. Alluri, B. Saravanakumar, S.-J. Kim, Flexible, hybrid piezoelectric film (BaTi_(1-x)Zr_xO₃)/PVDF nanogenerator as a self-powered fluid velocity sensor, *ACS Appl. Mater. Interfaces* 7 (18) (2015) 9831–9840, <https://doi.org/10.1021/acsm.5b01760>.
- [109] S. Cho, J.S. Lee, J. Jang, Enhanced crystallinity, dielectric, and energy harvesting performances of surface-treated barium titanate hollow nanospheres/PVDF nanocomposites, *Adv. Mater. Interfaces* 2 (10) (2015), 1500098, <https://doi.org/10.1002/admi.201500098>.
- [110] G.G. Genchi, A. Marino, A. Rocca, V. Mattoli, G. Ciofani, Barium titanate nanoparticles: promising multitasking vectors in nanomedicine, *Nanotechnology* 27 (23) (2016), 232001, <https://doi.org/10.1088/0957-4484/27/23/232001>.
- [111] S. Siddiqui, D.I. Kim, L.T. Duy, M.T. Nguyen, S. Muhammad, W.S. Yoon, N.E. Lee, High-performance flexible lead-free nanocomposite piezoelectric nanogenerator for biomechanical energy harvesting and storage, *Nano Energy* 15 (2015) 177–185, <https://doi.org/10.1016/j.nanoen.2015.04.030>.
- [112] S. Siddiqui, D.I. Kim, E. Roh, L.T. Duy, T.Q. Trung, M.T. Nguyen, N.E. Lee, A durable and stable piezoelectric nanogenerator with nanocomposite nanofibers embedded in an elastomer under high loading for a self-powered sensor system, *Nano Energy* 30 (2016) 434–442, <https://doi.org/10.1016/j.nanoen.2016.10.034>.
- [113] C. Shuai, G. Liu, Y. Yang, W. Yang, C. He, G. Wang, Z. Liu, F. Qi, S. Peng, Functionalized BaTiO₃ enhances piezoelectric effect towards cell response of bone scaffold, *Colloids Surf. B Biointerfaces* 185 (2020), 110587, <https://doi.org/10.1016/j.colsurfb.2019.110587>.
- [114] C. Shuai, et al., A strawberry-like Ag-decorated barium titanate enhances piezoelectric and antibacterial activities of polymer scaffold, *Nano Energy* 74 (2020), 104825, <https://doi.org/10.1016/j.nanoen.2020.104825>.
- [115] S. Harstad, N. D’Souza, N. Soin, A.A. El-Gendy, S. Gupta, V.K. Pecharsky, T. Shah, E. Siories, R.L. Hadimani, Enhancement of β-phase in PVDF films embedded with ferromagnetic Gd₅Si₄ nanoparticles for piezoelectric energy harvesting, *AIP Adv.* 7 (5) (2017), 056411, <https://doi.org/10.1063/1.4973596>.
- [116] H.B. Kang, C.S. Han, J.C. Pyun, W.H. Ryu, C.Y. Kang, Y.S. Cho, (Na,K)NbO₃ nanoparticle-embedded piezoelectric nanofiber composites for flexible nanogenerators, *Compos. Sci. Technol.* 111 (2015) 1–8, <https://doi.org/10.1016/j.compscitech.2015.02.015>.
- [117] N. Levi, R. Czerw, S. Xing, P. Iyer, D.L. Carroll, Properties of polyvinylidene difluoride–carbon nanotube blends, *Nano Lett* 4 (7) (2004) 1267–1271, <https://doi.org/10.1021/nl0494203>.
- [118] G.H. Kim, S.M. Hong, Y. Seo, Piezoelectric properties of poly(vinylidene fluoride) and carbon nanotube blends: β-phase development, *Phys. Chem. Chem. Phys.* 11 (44) (2009) 10506, <https://doi.org/10.1039/b912801h>.
- [119] H. Yu, T. Huang, M. Lu, M. Mao, Q. Zhang, H. Wang, Enhanced power output of an electrospun PVDF/MWCNTs-based nanogenerator by tuning its conductivity, *Nanotechnology* 24 (40) (2013), 405401, <https://doi.org/10.1088/0957-4484/24/40/405401>.
- [120] Y. Ahn, J.Y. Lim, S.M. Hong, J. Lee, J. Ha, H.J. Choi, Y. Seo, Enhanced piezoelectric properties of electrospun poly(vinylidene fluoride)/multiwalled carbon nanotube composites due to high β-phase formation in poly(vinylidene fluoride), *J. Phys. Chem. C* 117 (22) (2013) 11791–11799, <https://doi.org/10.1021/jp4011026>.
- [121] M. Sharma, V. Srinivas, G. Madras, S. Bose, Outstanding dielectric constant and piezoelectric coefficient in electrospun nanofiber mats of PVDF containing silver decorated multiwall carbon nanotubes: assessing through piezoresponse force microscopy, *RSC Adv.* 6 (8) (2016) 6251–6258, <https://doi.org/10.1039/C5RA25671B>.
- [122] Y.K. Fuh, C.C. Kuo, Z.M. Huang, S.C. Li, E.R. Liu, A transparent and flexible graphene-piezoelectric fiber generator, *Small* 12 (14) (2016) 1875–1881, <https://doi.org/10.1002/smll.201503605>.
- [123] V. Bhavanasi, V. Kumar, K. Parida, J. Wang, P.S. Lee, Enhanced piezoelectric energy harvesting performance of flexible PVDF-TrFE bilayer films with graphene oxide, *ACS Appl. Mater. Interfaces* 8 (1) (2016) 521–529, <https://doi.org/10.1021/acsm.5b09502>.
- [124] M. Ataur Rahman, B.-C. Lee, D.-T. Phan, G.-S. Chung, Fabrication and characterization of highly efficient flexible energy harvesters using PVDF-graphene nanocomposites, *Smart Mater. Struct.* 22 (8) (2013), 085017, <https://doi.org/10.1088/0964-1726/22/8/085017>.
- [125] Alamusi, J. Xue, L. Wu, N. Hu, J. Qiu, C. Chang, S. Atobe, H. Fukunaga, T. Watanabe, Y. Liu, H. Ning, J. Li, Y. Li, Y. Zhao, Evaluation of piezoelectric property of reduced graphene oxide (rGO)-poly(vinylidene fluoride) nanocomposites, *Nanoscale* 4 (22) (2012) 7250, <https://doi.org/10.1039/c2nr32185h>.
- [126] L. Feng, L. Wu, X. Qu, New horizons for diagnostics and therapeutic applications of graphene and graphene oxide, *Adv. Mater.* 25 (2) (2013) 168–186, <https://doi.org/10.1002/adma.201203229>.
- [127] L. Wu, W. Yuan, N. Hu, Z. Wang, C. Chen, J. Qiu, J. Ying, Y. Li, Improved piezoelectricity of PVDF-HFP/carbon black composite films, *J. Phys. D Appl. Phys.* 47 (13) (2014), 135302, <https://doi.org/10.1088/0022-3727/47/13/135302>.
- [128] B. Li, J. Zheng, C. Xu, Silver nanowire dopant enhancing piezoelectricity of electrospun PVDF nanofiber web, in: SPIE Proceedings, 2013, 879314. doi: 10.1117/12.2026758.
- [129] M.M. Alam, D. Mandal, Native cellulose microfiber-based hybrid piezoelectric generator for mechanical energy harvesting utility, *ACS Appl. Mater. Interfaces* 8 (3) (2016) 1555–1558, <https://doi.org/10.1021/acsm.5b08168>.
- [130] V. Bhavanasi, V. Kumar, K. Parida, J. Wang, P.S. Lee, Enhanced piezoelectric energy harvesting performance of flexible PVDF-TrFE bilayer films with graphene oxide, *ACS Appl. Mater. Interfaces* 8 (1) (2016) 521–529, <https://doi.org/10.1021/acsm.5b09502>.
- [131] D. Singh, A. Choudhary, A. Garg, Flexible and robust piezoelectric polymer nanocomposites based energy harvesters, *ACS Appl. Mater. Interfaces* 10 (3) (2018) 2793–2800, <https://doi.org/10.1021/acsm.7b16973>.
- [132] P. Thakur, A. Kool, N.A. Hoque, B. Bagchi, F. Khatun, P. Biswas, D. Brahma, S. Roy, S. Banerjee, S. Das, Superior performances of in situ synthesized ZnO/PVDF thin film based self-poled piezoelectric nanogenerator and self-charged photo-power bank with high durability, *Nano Energy* 44 (2018) 456–467, <https://doi.org/10.1016/j.nanoen.2017.11.065>.
- [133] M. Choi, G. Murillo, S. Hwang, J.W. Kim, J.H. Jung, C.Y. Chen, M. Lee, Mechanical and electrical characterization of PVDF-ZnO hybrid structure for application to nanogenerator, *Nano Energy* 33 (2017) 462–468, <https://doi.org/10.1016/j.nanoen.2017.01.062>.
- [134] B. Dutta, E. Kar, N. Bose, S. Mukherjee, NiO@SiO₂/PVDF: a flexible polymer nanocomposite for a high performance human body motion-based energy harvester and tactile e-skin mechanosensor, *ACS Sustain. Chem. Eng.* 6 (8) (2018) 10505–10516, <https://doi.org/10.1021/acssuschemeng.8b01851>.
- [135] M.M. Alam, A. Sultana, D. Mandal, Biomechanical and acoustic energy harvesting from TiO₂ nanoparticle modulated PVDF nanofiber made high performance nanogenerator, *ACS Appl. Energy Mater.* 1 (7) (2018) 3103–3112, <https://doi.org/10.1021/acsaem.8b00216>.
- [136] X. Ren, H. Fan, Y. Zhao, Z. Liu, Flexible lead-free BiFeO₃/PDMS-based nanogenerator as piezoelectric energy harvester, *ACS Appl. Mater. Interfaces* 8 (39) (2016) 26190–26197, <https://doi.org/10.1021/acsm.6b04497>.
- [137] H. Kim, S.M. Kim, H. Son, H. Kim, B. Park, J. Ku, J.I. Sohn, K. Im, J.E. Jang, J. J. Park, O. Kim, S. Cha, Y.J. Park, Enhancement of piezoelectricity via electrostatic effects on a textile platform, *Energy Environ. Sci.* 5 (10) (2012) 8932–8936, <https://doi.org/10.1039/c2ee22744d>.
- [138] S.K. Karan, S. Maiti, O. Kwon, S. Paria, A. Maitra, S.K. Si, Y. Kim, J.K. Kim, B. B. Khatau, Nature driven spider silk as high energy conversion efficient bio-piezoelectric nanogenerator, *Nano Energy* 49 (2018) 655–666, <https://doi.org/10.1016/j.nanoen.2018.05.014>.
- [139] Y. Zhang, C.K. Jeong, T. Yang, H. Sun, L.Q. Chen, S. Zhang, W. Chen, Q. Wang, Bioinspired elastic piezoelectric composites for high-performance mechanical energy harvesting, *J. Mater. Chem. A* 6 (30) (2018) 14546–14552, <https://doi.org/10.1039/c8ta03617a>.
- [140] Q. Zheng, H. Zhang, H. Mi, Z. Cai, Z. Ma, S. Gong, High-performance flexible piezoelectric nanogenerators consisting of porous cellulose nanofibril (CNF)/poly(dimethylsiloxane) (PDMS) aerogel films, *Nano Energy* 26 (2016) 504–512, <https://doi.org/10.1016/j.nanoen.2016.06.009>.
- [141] S. Maiti, S. Kumar Karan, J. Lee, A. Kumar Mishra, B. Bhushan Khatua, J. Kon Kim, Bio-waste onion skin as an innovative nature-driven piezoelectric material with high energy conversion efficiency, *Nano Energy* 42 (2017) 282–293, <https://doi.org/10.1016/j.nanoen.2017.10.041>.
- [142] S.K. Ghosh, D. Mandal, Efficient natural piezoelectric nanogenerator: electricity generation from fish swim bladder, *Nano Energy* 28 (2016) 356–365, <https://doi.org/10.1016/j.nanoen.2016.08.030>.
- [143] S.K. Karan, S. Maiti, S. Paria, A. Maitra, S.K. Si, J.K. Kim, B.B. Khatau, A new insight towards eggshell membrane as high energy conversion efficient bio-piezoelectric energy harvester, *Mater. Today Energy* 9 (2018) 114–125, <https://doi.org/10.1016/j.mtener.2018.05.006>.
- [144] N.R. Alluri, N.P. Maria Joseph Raj, G. Khandelwal, V. Vivekananthan, S.J. Kim, Aloe vera: a tropical desert plant to harness the mechanical energy by triboelectric and piezoelectric approaches, *Nano Energy* 73 (2020), 104767, <https://doi.org/10.1016/j.nanoen.2020.104767>.
- [145] S. Luo, J. Zhao, J. Zou, Z. He, C. Xu, F. Liu, Y. Huang, L. Dong, L. Wang, H. Zhang, Self-standing polypyrrole/black phosphorus laminated film: promising electrode for flexible supercapacitor with enhanced capacitance and cycling stability, *ACS Appl. Mater. Interfaces* 10 (4) (2018) 3538–3548, <https://doi.org/10.1021/acsm.7b15458>.

- [146] X. Qi, Y. Zhang, Q. Ou, S.T. Ha, C.W. Qiu, H. Zhang, Y.B. Cheng, Q. Xiong, Q. Bao, Photonics and optoelectronics of 2D metal-halide perovskites, *Small* 14 (31) (2018), 1800682, <https://doi.org/10.1002/smll.201800682>.
- [147] M. Qiu, Z.T. Sun, D.K. Sang, X.G. Han, H. Zhang, C.M. Niu, Current progress in black phosphorus materials and their applications in electrochemical energy storage, *Nanoscale* 9 (36) (2017) 13384–13403, <https://doi.org/10.1039/C7NR03318D>.
- [148] J. Pei, J. Yang, T. Yildirim, H. Zhang, Y. Lu, Many-body complexes in 2D semiconductors, *Adv. Mater.* 31 (2) (2019), 1706945, <https://doi.org/10.1002/adma.201706945>.
- [149] D. Ma, Y. Li, H. Mi, S. Luo, P. Zhang, Z. Lin, J. Li, H. Zhang, Robust SnO₂–x nanoparticle-impregnated carbon nanofibers with outstanding electrochemical performance for advanced sodium-ion batteries, *Angew. Chem. Int. Ed.* 57 (29) (2018) 8901–8905, <https://doi.org/10.1002/anie.201802672>.
- [150] X. Chen, G. Xu, X. Ren, Z. Li, X. Qi, K. Huang, H. Zhang, Z. Huang, J. Zhong, A black/red phosphorus hybrid as an electrode material for high-performance Li-ion batteries and supercapacitors, *J. Mater. Chem. A* 5 (14) (2017) 6581–6588, <https://doi.org/10.1039/C7TA00455A>.
- [151] X. Jiang, A.V. Kuklin, A. Baev, Y. Ge, H. Ågren, H. Zhang, P.N. Prasad, Two-dimensional MXenes: from morphological to optical, electric, and magnetic properties and applications, *Phys. Rep.* 848 (2020) 1–58, <https://doi.org/10.1016/j.physrep.2019.12.006>.
- [152] J. He, L. Tao, H. Zhang, B. Zhou, J. Li, Emerging 2D materials beyond graphene for ultrashort pulse generation in fiber lasers, *Nanoscale* 11 (6) (2019) 2577–2593, <https://doi.org/10.1039/C8NR09368G>.
- [153] S. Guo, Y. Zhang, Y. Ge, S. Zhang, H. Zeng, H. Zhang, 2D V-V binary materials: status and challenges, *Adv. Mater.* 31 (39) (2019), 1902352, <https://doi.org/10.1002/adma.201902352>.
- [154] N. Sezer, S.A. Khan, M. Koç, Boiling heat transfer enhancement by self-assembled graphene/silver hybrid film for the thermal management of concentrated photovoltaics, *Energy Technol.* (2020), 2000532, <https://doi.org/10.1002/ente.202000532>.
- [155] S.A. Khan, N. Sezer, M. Koç, Design, synthesis, and characterization of hybrid micro-nano surface coatings for enhanced heat transfer applications, *Int. J. Energy Res.* (2020) er.5685, <https://doi.org/10.1002/er.5685>.
- [156] S.A. Khan, N. Sezer, M. Koç, Design, fabrication and nucleate pool-boiling heat transfer performance of hybrid micro-nano scale 2-D modulated porous surfaces, *Appl. Therm. Eng.* 153 (2019) 168–180, <https://doi.org/10.1016/j.applthermaleng.2019.02.133>.
- [157] S.A. Khan, N. Sezer, S. Ismail, M. Koç, Design, synthesis and nucleate boiling performance assessment of hybrid micro-nano porous surfaces for thermal management of concentrated photovoltaics (CPV), *Energy Convers. Manag.* 195 (2019) 1056–1066, <https://doi.org/10.1016/j.enconman.2019.05.068>.
- [158] N. Sezer, S.A. Khan, M. Koç, Amelioration of the pool boiling heat transfer performance via self- assembling of 3D porous graphene/carbon nanotube hybrid film over the heating surface, *Int. J. Heat Mass Transf.* 145 (118732) (2019) 1–12, <https://doi.org/10.1016/j.ijheatmasstransfer.2019.118732>.
- [159] N. Sezer, S.A. Khan, M. Koç, Amelioration of the pool boiling heat transfer performance by colloidal dispersions of carbon black, *Int. J. Heat Mass Transf.* 137 (2019) 599–608, <https://doi.org/10.1016/j.ijheatmasstransfer.2019.03.161>.
- [160] N. Sezer, M.A. Atieh, M. Koç, A comprehensive review on synthesis, stability, thermophysical properties, and characterization of nanofluids, *Powder Technol.* 344 (2018) 404–431, <https://doi.org/10.1016/j.powtec.2018.12.016>.
- [161] N. Sezer, M. Koç, Oxidative acid treatment of carbon nanotubes, *Surf. Interfaces* 14 (2018) 1–8, <https://doi.org/10.1016/j.surfin.2018.11.001>.
- [162] R. Li, Y. Yu, B. Zhou, Q. Guo, M. Li, J. Pei, Harvesting energy from pavement based on piezoelectric effects: fabrication and electric properties of piezoelectric vibrator, *J. Renew. Sustain. Energy* 10 (5) (2018) 1–11, <https://doi.org/10.1063/1.5002731>.
- [163] A. Moure, M.A. Izquierdo Rodríguez, S.H. Rueda, A. Gonzalo, F. Rubio-Marcos, D. U. Cuadros, A. Pérez-Lepe, J.F. Fernández, Feasible integration in asphalt of piezoelectric cymbals for vibration energy harvesting, *Energy Convers. Manag.* 112 (2016) 246–253, <https://doi.org/10.1016/j.enconman.2016.01.030>.
- [164] Y. Song, C.H. Yang, S.K. Hong, S.J. Hwang, J.H. Kim, J.Y. Choi, S.K. Ryu, T. H. Sung, Road energy harvester designed as a macro-power source using the piezoelectric effect, *Int. J. Hydron. Energy* 41 (29) (2016) 12563–12568, <https://doi.org/10.1016/j.ijhydene.2016.04.149>.
- [165] I. Jung, Y.H. Shin, S. Kim, J. young Choi, C.Y. Kang, Flexible piezoelectric polymer-based energy harvesting system for roadway applications, *Appl. Energy* 197 (2017) 222–229, <https://doi.org/10.1016/j.apenergy.2017.04.020>.
- [166] M. Khalili, A.B. Biten, G. Vishwakarma, S. Ahmed, A.T. Papagiannakis, Electromechanical characterization of a piezoelectric energy harvester, *Appl. Energy* 253 (2019), 113585, <https://doi.org/10.1016/j.apenergy.2019.113585>.
- [167] M.Y. Gao, P. Wang, Y. Cao, R. Chen, C. Liu, A rail-borne piezoelectric transducer for energy harvesting of railway vibration, *J. Vibroeng.* 18 (7) (2016) 4647–4663, <https://doi.org/10.2159/jve.2016.16938>.
- [168] N. Bosso, M. Magelli, N. Zampieri, Application of low-power energy harvesting solutions in the railway field: a review, *Veh. Syst. Dyn.* (2020) 1–31, <https://doi.org/10.1080/00423114.2020.1726973>.
- [169] M. Karimi, A.H. Karimi, R. Tikani, S. Ziaeii-Rad, Experimental and theoretical investigations on piezoelectric-based energy harvesting from bridge vibrations under travelling vehicles, *Int. J. Mech. Sci.* 119 (2016).
- [170] H. Wang, A. Jasim, X. Chen, Energy harvesting technologies in roadway and bridge for different applications – a comprehensive review, *Appl. Energy* 212 (2018) 1083–1094, <https://doi.org/10.1016/j.apenergy.2017.12.125>.
- [171] N. Chen, H.J. Jung, H. Jabbar, T.H. Sung, T. Wei, A piezoelectric impact-induced vibration cantilever energy harvester from speed bump with a low-power power management circuit, *Sens. Actuators A Phys.* 254 (2017) 134–144, <https://doi.org/10.1016/j.sna.2016.12.006>.
- [172] G. del Castillo-García, E. Blanco-Fernandez, P. Pascual-Muñoz, D. Castro-Fresno, Energy harvesting from vehicular traffic over speed bumps: a review, *Proc. Inst. Civ. Eng. Energy* 171 (2) (2018) 58–69, <https://doi.org/10.1680/jener.17.00008>.
- [173] W. Hendrowati, H.L. Guntur, I.N. Sutantra, Design, modeling and analysis of implementing a multilayer piezoelectric vibration energy harvesting mechanism in the vehicle suspension, *Engineering* 04 (11) (2012) 728–738, <https://doi.org/10.4236/eng.2012.411094>.
- [174] J. Lee, J. Oh, H. Kim, B. Choi, Strain-based piezoelectric energy harvesting for wireless sensor systems in a tire, *J. Intell. Mater. Syst. Struct.* 26 (11) (2015) 1404–1416, <https://doi.org/10.1177/1045389X14544138>.
- [175] R. Esmaeili, H. Aliniagerdroudbari, S.R. Hashemi, A. Nazari, M. Alhadri, W. Zakri, A.H. Mohammed, C. Batur, S. Farhad, A rainbow piezoelectric energy harvesting system for intelligent tire monitoring applications, *J. Energy Resour. Technol.* 141 (6) (2019), <https://doi.org/10.1115/1.4042398>.
- [176] C.R. Bowen, M.H. Arafa, Energy harvesting technologies for tire pressure monitoring systems, *Adv. Energy Mater.* 5 (7) (2015), 1401787, <https://doi.org/10.1002/entm.201401787>.
- [177] G.W. Kim, Piezoelectric energy harvesting from torsional vibration in internal combustion engines, *Int. J. Automot. Technol.* 16 (4) (2015) 645–651, <https://doi.org/10.1007/s12239>.
- [178] M.A.A. Abdulkareem, L. Xu, M. Ali, A. Elagouz, J. Mi, S. Guo, Y. Liu, L. Zuo, Vibration energy harvesting in automotive suspension system: a detailed review, *Appl. Energy* 229 (2018) 672–699, <https://doi.org/10.1016/j.apenergy.2018.08.030>.
- [179] K.B. Kim, J.Y. Cho, H. Jabbar, J.H. Ahn, S.D. Hong, S.B. Woo, T.H. Sung, Optimized composite piezoelectric energy harvesting floor tile for smart home energy management, *Energy Convers. Manag.* 171 (2018) 31–37, <https://doi.org/10.1016/j.enconman.2018.05.031>.
- [180] O. Puscasu, N. Counsell, M.R. Herfatmanesh, R. Peace, J. Patsavellas, R. Day, Powering lights with piezoelectric energy-harvesting floors, *Energy Technol.* 6 (2018) 1–12.
- [181] F. Petriti, K. Gkounas, Piezoelectric energy harvesting from vortex shedding and galloping induced vibrations inside HVAC ducts, *Energy Build.* 158 (2018) 371–383, <https://doi.org/10.1016/j.enbuild.2017.09.099>.
- [182] S. Orrego, K. Shoele, A. Ruas, K. Doran, B. Caggiano, R. Mittal, S.H. Kang, Harvesting ambient wind energy with an inverted piezoelectric flag, *Appl. Energy* 194 (2017) 212–222, <https://doi.org/10.1016/j.apenergy.2017.03.016>.
- [183] G.W. Taylor, J.R. Burns, S.M. Kammann, W.B. Powers, T.R. Welsh, The energy harvesting Eel: a small subsurface ocean/river power generator, *IEEE J. Ocean. Eng.* 26 (4) (2001) 539–547, <https://doi.org/10.1109/48.972090>.
- [184] A. Erturk, G. Delporte, Underwater thrust and power generation using flexible piezoelectric composites: an experimental investigation toward self-powered swimmer-sensor platforms, *Smart Mater. Struct.* 20 (12) (2011), 125013, <https://doi.org/10.1088/0964-1726/20/12/125013>.
- [185] Y. Cha, H. Kim, M. Porfirio, Energy harvesting from underwater base excitation of a piezoelectric composite beam, *Smart Mater. Struct.* 22 (11) (2013), 115026, <https://doi.org/10.1088/0964-1726/22/11/115026>.
- [186] D.-A. Wang, N.-Z. Liu, A shear mode piezoelectric energy harvester based on a pressurized water flow, *Sens. Actuators A Phys.* 167 (2) (2011) 449–458, <https://doi.org/10.1016/j.sna.2011.03.003>.
- [187] K.A. Cunefare, N. Verma, A. Erturk, E. Skow, J. Savor, M. Cacan, Energy harvesting from hydraulic pressure fluctuations, in: vol. 2 Mechanics and Behavior of Active Materials; Integrated System Design and Implementation; Bio-Inspired Materials and Systems; Energy Harvesting, 2012, 729–738 doi: 10.1115/SMAS2012-7926.
- [188] Y. Cha, W. Chae, H. Kim, H. Walcott, S.D. Peterson, M. Porfirio, Energy harvesting from a piezoelectric biomimetic fish tail, *Renew. Energy* 86 (2016) 449–458, <https://doi.org/10.1016/j.renene.2015.07.077>.
- [189] S.F. Nabavi, A. Farshidianfar, A. Afsharfard, H.H. Khodaparast, An ocean wave-based piezoelectric energy harvesting system using breaking wave force, *Int. J. Mech. Sci.* 151 (2019) 498–507, <https://doi.org/10.1016/j.ijmecsci.2018.12.008>.
- [190] W.S. Hwang, J.H. Ahn, S.Y. Jeong, H.J. Jung, S.K. Hong, J.Y. Choi, J.Y. Cho, J. H. Kim, T.H. Sung, Design of piezoelectric ocean-wave energy harvester using sway movement, *Sens. Actuators A Phys.* 260 (2017) 191–197, <https://doi.org/10.1016/j.sna.2017.04.026>.
- [191] Z. Wang, L. Tan, X. Pan, G. Liu, Y. He, W. Jin, M. Li, Y. Hu, H. Gu, Self-powered viscosity and pressure sensing in microfluidic systems based on the piezoelectric energy harvesting of flowing droplets, *ACS Appl. Mater. Interfaces* 9 (34) (2017) 28586–28595, <https://doi.org/10.1021/acsami.7b08541>.
- [192] I. Izadgoshasb, Y.Y. Lim, N. Lake, L. Tang, R.V. Padilla, T. Kashiwao, Optimizing orientation of piezoelectric cantilever beam for harvesting energy from human walking, *Energy Convers. Manag.* 161 (2018) 66–73, <https://doi.org/10.1016/j.enconman.2018.01.076>.
- [193] K.B. Kim, W. Jang, J.Y. Cho, S.B. Woo, D.H. Jeon, J.H. Ahn, S.D. Hong, H.Y. Koo, T.H. Sung, Transparent and flexible piezoelectric sensor for detecting human movement with a boron nitride nanosheet (BNNS), *Nano Energy* 54 (2018) 91–98, <https://doi.org/10.1016/j.nanoen.2018.09.056>.
- [194] W.S. Jung, M.J. Lee, M.G. Kang, H.G. Moon, S.J. Yoon, S.H. Baek, C.Y. Kang, Powerful curved piezoelectric generator for wearable applications, *Nano Energy* 13 (2015) 174–181, <https://doi.org/10.1016/j.nanoen.2015.01.051>.

- [195] K. Fan, Z. Liu, H. Liu, L. Wang, Y. Zhu, B. Yu, Scavenging energy from human walking through a shoe-mounted piezoelectric harvester, *Appl. Phys. Lett.* 110 (14) (2017), 143902, <https://doi.org/10.1063/1.4979832>.
- [196] E.M. Nia, N.A.W.A. Zawawi, B.S.M. Singh, A review of walking energy harvesting using piezoelectric materials, *IOP Conf. Ser. Mater. Sci. Eng.* 291 (2017), 012026, <https://doi.org/10.1088/1757-899X/291/1/012026>.
- [197] A.C. Turkmen, C. Celik, Energy harvesting with the piezoelectric material integrated shoe, *Energy* 150 (2018) 556–564, <https://doi.org/10.1016/j.energy.2017.12.159>.
- [198] S.J. Hwang, H.J. Jung, J.H. Kim, J.H. Ahn, D. Song, Y. Song, H.L. Lee, S.P. Moon, H. Park, T.H. Sung, Designing and manufacturing a piezoelectric tile for harvesting energy from footsteps, *Curr. Appl. Phys.* 15 (6) (2015) 669–674, <https://doi.org/10.1016/j.cap.2015.02.009>.
- [199] W. Deng, T. Yang, L. Jin, C. Yan, H. Huang, X. Chu, Z. Wang, D. Xiong, G. Tian, Y. Gao, H. Zhang, W. Yang, Cowpea-structured PVDF/ZnO nanofibers based flexible self-powered piezoelectric bending motion sensor towards remote control of gestures, *Nano Energy* 55 (2019) 516–525, <https://doi.org/10.1016/j.nanoen.2018.10.049>.
- [200] L. Zhao, H. Li, J. Meng, Z. Li, The recent advances in self-powered medical information sensors, *InfoMat* 2 (1) (2020) 212–234, <https://doi.org/10.1002/inf2.12064>.
- [201] L. Dong, et al., Invivo cardiac power generation enabled by an integrated helical piezoelectricpacemaker lead, *Nano Energy* 66 (2019), 104085, <https://doi.org/10.1016/j.nanoen.2019.104085>.
- [202] H. Zhang, X.S. Zhang, X. Cheng, Y. Liu, M. Han, X. Xue, S. Wang, F. Yang, S. A. S. H. Zhang, Z. Xu, A flexible and implantable piezoelectric generator harvesting energy from the pulsation of ascending aorta: in vitro and in vivo studies, *Nano Energy* 12 (2015) 296–304, <https://doi.org/10.1016/j.nanoen.2014.12.038>.
- [203] L. Jiang, Y. Yang, R. Chen, G. Lu, R. Li, D. Li, M.S. Humayun, K.K. Shung, J. Zhu, Y. Chen, Q. Zhou, Flexible piezoelectric ultrasonic energy harvester array for bio-implantable wireless generator, *Nano Energy* 56 (2019) 216–224, <https://doi.org/10.1016/j.nanoen.2018.11.052>.
- [204] M. Southcott, K. MacVittie, J. Halámková, W.D. Jemison, R. Lobel, E. Katz, A pacemaker powered by an implantable biofuel cell operating under conditions mimicking the human blood circulatory system – battery not included, *Phys. Chem. Chem. Phys.* 15 (17) (2013) 6278, <https://doi.org/10.1039/c3cp50929j>.
- [205] N. Li, Z. Yi, Y. Ma, F. Xie, Y. Huang, Y. Tian, X. Dong, Y. Liu, X. Shao, Y. Li, L. Jin, J. Liu, Z. Xu, B. Yang, H. Zhang, Direct powering a real cardiac pacemaker by natural energy of a heartbeat, *ACS Nano* 13 (3) (2019) 2822–2830, <https://doi.org/10.1021/acsnano.8b08567>.
- [206] G.-T. Hwang, H. Park, J.H. Lee, S. Oh, K.I. Park, M. Byun, H. Park, G. Ahn, C. K. Jeong, K. No, H. Kwon, S.G. Lee, B. Joung, K.J. Lee, Self-powered cardiac pacemaker enabled by flexible single crystalline PMN-PT piezoelectric energy harvester, *Adv. Mater.* 26 (28) (2014) 4880–4887, <https://doi.org/10.1002/adma.201400562>.
- [207] M.H. Ansari, M.A. Karami, Piezoelectric energy harvesting from heartbeat vibrations for leadless pacemakers, *J. Phys. Conf. Ser.* 660 (1) (2015), 012121, <https://doi.org/10.1088/1742-6596/660/1/012121>.
- [208] D.H. Kim, H.J. Shin, H. Lee, C.K. Jeong, H. Park, G.T. Hwang, H.Y. Lee, D.J. Joe, J.H. Han, S.H. Lee, J. Kim, B. Joung, K.J. Lee, In vivo self-powered wireless transmission using biocompatible flexible energy harvesters, *Adv. Funct. Mater.* 27 (25) (2017), 1700341, <https://doi.org/10.1002/adfm.201700341>.
- [209] O.T. Inan, P.F. Migeotte, K.S. Park, M. Etemadi, K. Tavakolian, R. Casanella, J. Zanetti, J. Tank, I. Funtova, G.K. Prisk, M. Di Renzo, Ballistocardiography and seismocardiography: a review of recent advances, *IEEE J. Biomed. Health Inform.* 19 (4) (2015) 1414–1427, <https://doi.org/10.1109/JBHI.2014.2361732>.
- [210] J. Ben-Ari, E. Zimlichman, N. Adi, P. Sorkine, Contactless respiratory and heart rate monitoring: validation of an innovative tool, *J. Med. Eng. Technol.* 34 (7–8) (2010) 393–398, <https://doi.org/10.3109/03091902.2010.503308>.
- [211] M. Migliorini, J.M. Kortelainen, J. Pärkkä, M. Tenhunen, S.L. Himanen, A. M. Bianchi, Monitoring nocturnal heart rate with bed sensor, *Methods Inf. Med.* 53 (4) (2014) 308–313, <https://doi.org/10.3414/ME13-02-0053>.
- [212] P.A. Heidenreich, J.G. Trogdon, O.A. Khavjou, J. Butler, K. Dracup, M. D. Ezekowitz, E.A. Finkelstein, Y. Hong, S.C. Johnston, A. Khera, D.M. Lloyd-Jones, S.A. Nelson, G. Nichol, D. Orenstein, P. Wilson, Y.J. Woo, Forecasting the future of cardiovascular disease in the United States, *Circulation* 123 (8) (2011) 933–944, <https://doi.org/10.1161/CIR.0b013e31820a5f5>.
- [213] L.Y. Chen, B. Tee, A.L. Chortos, G. Schwartz, V. Tse, D. J. Lipomi, H. Wong, M. V. McConnell, Z. Bao, Continuous wireless pressure monitoring and mapping with ultra-small passive sensors for health monitoring and critical care, *Nat. Commun.* 5 (1) (2014) 5028, <https://doi.org/10.1038/ncomms6028>.
- [214] C. Dagdeviren, Z. Li, Z.L. Wang, Energy harvesting from the animal/human body for self-powered electronics, *Annu. Rev. Biomed. Eng.* 19 (1) (2017) 85–108, <https://doi.org/10.1146/annurev-bioeng-071516-044517>.
- [215] X. Cheng, X. Xue, Y. Ma, M. Han, W. Zhang, Z. Xu, H. Zhang, H. Zhang, Implantable and self-powered blood pressure monitoring based on a piezoelectric thinfilm: simulated, in vitro and in vivo studies, *Nano Energy* 22 (2016) 453–460, <https://doi.org/10.1016/j.nanoen.2016.02.037>.
- [216] J. Yang, J. Chen, Y. Su, Q. Jing, Z. Li, F. Yi, X. Wen, Z. Wang, Z.L. Wang, Eardrum-inspired active sensors for self-powered cardiovascular system characterization and throat-attached anti-interference voice recognition, *Adv. Mater.* 27 (8) (2015) 1316–1326, <https://doi.org/10.1002/adma.201404794>.
- [217] C.M. Boutry, A. Nguyen, Q.O. Lawal, A. Chortos, S. Rondeau-Gagné, Z. Bao, A sensitive and biodegradable pressure sensor array for cardiovascular monitoring, *Adv. Mater.* 27 (43) (2015) 6954–6961, <https://doi.org/10.1002/adma.201502535>.
- [218] T. Yamaguchi, D. Yamamoto, T. Arie, S. Akita, K. Takei, Wrist flexible heart pulse sensor integrated with a soft pump and a pneumatic balloon membrane, *RSC Adv.* 10 (29) (2020) 17353–17358, <https://doi.org/10.1039/DORA02316G>.
- [219] D.Y. Park, D.J. Joe, D.H. Kim, H. Park, J.H. Han, C.K. Jeong, H. Park, J.G. Park, B. Joung, K.J. Lee, Self-powered real-time arterial pulse monitoring using ultrathin epidermal piezoelectric sensors, *Adv. Mater.* 29 (37) (2017), 1702308, <https://doi.org/10.1002/adma.201702308>.
- [220] H. Ouyang, J. Tian, G. Sun, Y. Zou, Z. Liu, H. Li, L. Zhao, B. Shi, Y. Fan, Y. Fan, Z. L. Wang, Z. Li, Self-powered pulse sensor for antidiastole of cardiovascular disease, *Adv. Mater.* 29 (40) (2017), 1703456, <https://doi.org/10.1002/adma.201703456>. Oct.
- [221] K. Meng, J. Chen, X. Li, Y. Wu, W. Fan, Z. Zhou, Q. He, X. Wang, X. Fan, Y. Zhang, J. Yang, Z.L. Wang, Flexible weaving constructed self-powered pressure sensor enabling continuous diagnosis of cardiovascular disease and measurement of cuffless blood pressure, *Adv. Funct. Mater.* (2018), 1806388, <https://doi.org/10.1002/adfm.201806388>.
- [222] G.T. Hwang, Y. Kim, J.H. Lee, S. Oh, C.K. Jeong, D.Y. Park, J. Ryu, H. Kwon, S. G. Lee, B. Joung, D. Kim, K.J. Lee, Self-powered deep brain stimulation via a flexible PIIMT energy harvester, *Energy Environ. Sci.* 8 (9) (2015) 2677–2684, <https://doi.org/10.1039/c5ee01593f>.
- [223] R. Fan, S. Lee, H. Jung, M.A. Melo, R. Masri, Piezoelectric energy harvester utilizing mandibular deformation to power implantable biosystems: a feasibility study, *J. Mech. Sci. Technol.* 33 (8) (2019) 4039–4045, <https://doi.org/10.1007/s12206-019-0749-4>.
- [224] J. Liu, H. Gu, Q. Liu, L. Ren, G. Li, An intelligent material for tissue reconstruction: the piezoelectric property of polycaprolactone/barium titanate composites, *Mater. Lett.* 236 (2019) 686–689, <https://doi.org/10.1016/j.matlet.2018.11.036>.
- [225] J. Jacob, N. More, K. Kalia, G. Kapusetti, Piezoelectric smart biomaterials for bone and cartilage tissue engineering, *Inflamm. Regen.* 38 (1) (2018) 1–11, <https://doi.org/10.1186/s41232-018-0059-8>.
- [226] A. Zaszczyńska, P. Sajkiewicz, A. Grady, Piezoelectric scaffolds as smart materials for neural tissue engineering, *Polymers* 12 (1) (2020) 161, <https://doi.org/10.3390/polym12010161>.
- [227] L.F. Jaffe, M.-M. Poo, Neurites grow faster towards the cathode than the anode in a steady field, *J. Exp. Zool.* 209 (1) (1979) 115–127, <https://doi.org/10.1002/jez.1402090114>.
- [228] N. Patel, M. Poo, Orientation of neurite growth by extracellular electric fields, *J. Neurosci.* 2 (4) (1982) 483–496, <https://doi.org/10.1523/JNEUROSCI.02-04-00483.1982>.
- [229] A. Bassett, R. Pawluk, R. Becker, Effects of electric currents on bone in vivo, *Nature* 495 (1964) 652–654.
- [230] T. Kobayashi, S. Nakamura, K. Yamashita, Enhanced osteobonding by negative surface charges of electrically polarized hydroxyapatite, *J. Biomed. Mater. Res.* 57 (4) (2001) 477–484, [https://doi.org/10.1002/1097-4636\(20011215\)57:4<477::AID-JBMR1193>3.0.CO;2-5](https://doi.org/10.1002/1097-4636(20011215)57:4<477::AID-JBMR1193>3.0.CO;2-5).



Nurettin Sezer is a postdoctoral research fellow in Sustainable Energy at Hamad Bin Khalifa University. He obtained his BSc degree at Hacettepe University and MSc degree at Middle East Technical University, Turkey in 2010 and 2013, respectively. He received his PhD degree from Hamad Bin Khalifa University, Qatar in 2019. He published +15 papers in reputable journals in the recent years. His research interests focus on energy harvesting, energy systems, renewable energy, energy efficiency, thermodynamics, system integration, system analysis, desalination, fuel cells, multigeneration, heat transfer, nanomaterials, nanofluids, nano energy, superparamagnetism, nano and micro-engineered surfaces, biodegradable materials, and tissue engineering.



Muammer Koç is a Founding Professor and Head of Sustainable Development Division at Hamad Bin Khalifa University. He obtained his BSc degree at Middle East Technical University, Turkey in 1991. Later, he received MSc and PhD degrees from The Ohio State University, OH, USA in 1996 and 1999, respectively. Besides, he obtained an Executive MBA degree from University of Sheffield, UK in 2014. He has authored and coauthored +200 scientific papers. His research interests focus on materials science, advanced manufacturing, heat and mass transfer, energy efficiency, energy policy, biomedical, tissue engineering, R&D and innovation policies, and education systems.